
HUMAN-IN-THE-LOOP ADAPTIVE OPTIMIZATION FOR IMPROVED TIME SERIES FORECASTING

000
001
002
003
004
005 **Anonymous authors**
006 Paper under double-blind review
007
008
009
010

ABSTRACT

011 Time-series forecasting models often produce *systematic* and predictable errors,
012 even in critical domains such as energy, finance, and healthcare. We introduce a
013 novel *post-training adaptive optimization* framework that improves forecast accu-
014 racy without retraining or architectural changes. Our approach adds a lightweight
015 model-agnostic correction layer that automatically finds expressive output trans-
016 formations optimized by reinforcement learning, contextual bandits, or genetic
017 algorithms. Theoretically, we prove the benefit of an affine correction and quantify
018 the expected performance gain together with its computational cost. The frame-
019 work also supports an *optional* human-in-the-loop component: domain experts
020 can guide corrections using natural language, which is parsed into actions by a
021 language model. Across multiple benchmarks (e.g. electricity, weather, traffic),
022 we observe consistent accuracy gains with minimal computational overhead. Our
023 interactive demo ([link](#)) showcases the usability of the framework in real time. By
024 combining automated post-hoc refinement with domain-expert corrections to the
025 base forecasting model, our approach offers a lightweight yet powerful direction
026 for practical forecasting systems.
027

1 INTRODUCTION

030 Time series forecasting is critical in domains such as finance (Krollner et al., 2010), health-
031 care (Kaushik et al., 2020), and energy management (Palma et al., 2024), where accurate predictions
032 drive high-stakes decisions. Although modern machine learning models have improved forecasting
033 performance, they still face two persistent limitations: (1) insufficient model expressiveness to cap-
034 ture complex, real-world patterns, and (2) difficulty incorporating domain expertise into predictions.
035 Traditional forecast pipelines (Meisenbacher et al., 2022) often rely on rigid architectures and static
036 assumptions, leading to systematic errors that domain experts can easily identify.

037 However, integrating expert feedback remains challenging: manual corrections are time consum-
038 ing, and existing methods (Geweke & Whiteman, 2006; Girard et al., 2002) require extensive
039 re-engineering or ensembling techniques (Khashei & Bijari, 2012). These limitations prevent models
040 from adapting effectively to changing environments.

041 To address these issues, we propose a flexible, lightweight *post-training optimization* framework that
042 improves forecasts without re-training the model. Our preliminary theoretical insight suggests the
043 opportunity for such a post hoc correction. Building on this, we extend post-training correction into
044 a broader optimization framework that adaptively adjusts model outputs using approaches such as
045 reinforcement learning, bandits, or genetic algorithms.

046 Our proposed approach, illustrated in [Figure 1](#) and [Figure 2](#), is scalable, model-agnostic and accessible
047 through an interactive web interface, making it practical for both researchers and practitioners.

048 Our novel approach introduces key features that distinguish it from previous work:

049

- 050 1. *Adaptive Model Augmentation*: Automatically identifies and applies expressive transfor-
051 mations that improve the performance of the forecast, expanding the model function class
052 without architectural changes.
- 053 2. *Human-in-the-Loop (HITL)*: *Optionally incorporates expert feedback, expressed in natural
language and safely translated into a post-training action code, which is further optimized*

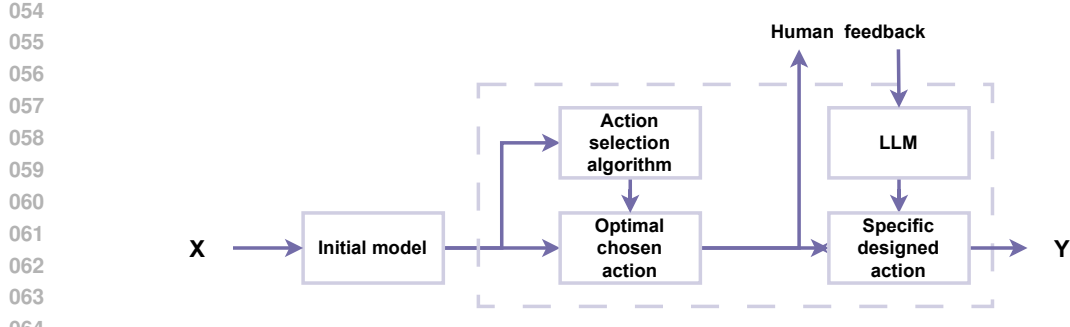


Figure 1: Overview of the forecasting pipeline: the initial model generates predictions from input X , which are refined by an action selection mechanism and optionally adjusted using human feedback interpreted by a language model (LLM), yielding the final output Y .

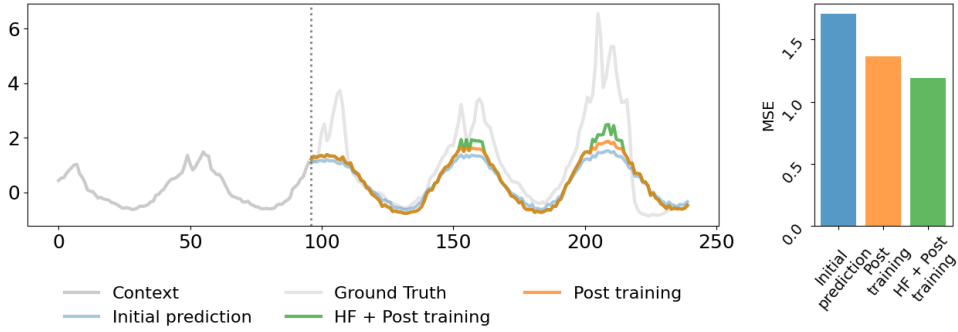


Figure 2: **(Left)** Ground truth, initial prediction, and corrected predictions produced by the proposed forecasting pipeline. The human feedback applied was: *“Increase values above a chosen quantile by 10% to 50%.”*. **(Right)** Performance comparison of the different predictions: the base forecast, the automatically corrected output, and the correction incorporating human feedback.

via reinforcement learning, bandit methods, or genetic algorithms to iteratively improve and refine forecasts.

2 RELATED WORK

Time Series Forecasting Models Time series forecasting has long been a fundamental task in statistical modeling. Traditional models such as ARIMA (Newbold, 1983), SARIMA (Korstanje, 2021), and ETS (Gardner Jr, 1985) work well for simple linear dynamics, but struggle with non-stationary or highly non-linear signals. Modern deep learning models, including LSTMs (Graves & Graves, 2012; Lin et al., 2023) and Transformers (Liu et al., 2023; Ilbert et al., 2024; Wu et al., 2021; Nie et al., 2023), offer improved expressiveness by learning long-range dependencies. Recent zero-shot models such as TimesFM (Das et al., 2024), Chronos (Ansari et al., 2024), and Lag-LLaMA (Rasul et al., 2023) further generalize across tasks via foundation model scaling. Despite these advances, existing models often exhibit systematic forecast errors and lack mechanisms to incorporate expert corrections.

Our work complements existing models by adding a post-training optimization layer that enhances performance without retraining and is compatible with any forecasting architecture.

Post-Training and Human Feedback in Forecasting Incorporating expert knowledge into forecasting has a long history, from manual tuning and domain-specific feature engineering (Tavenard et al., 2020; Zhou, 2020; Verkade et al., 2013; Madadgar et al., 2014) to judgmental forecasting methods (Armstrong, 1986; Bunn & Wright, 1991; Webby & O’Connor, 1996). However, such methods are typically manual, hard to scale, and not integrated into learning pipelines. Recent work

108
109
110
111
112
113
114
115
116
117
118
119
120
121
122
123
124
125
126
127
128
129
130
131
132
133
134
135
136
137
138
139
140
141
142
143
144
145
146
147
148
149
150
151
152
153
154
155
156
157
158
159
160
161

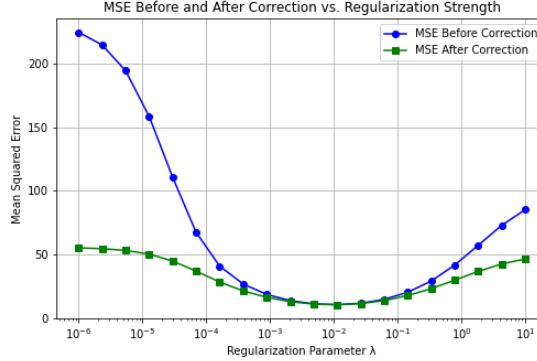


Figure 3: Illustration of the effect of affine post-training correction on ridge regression forecasts. The model is trained on a synthetic linear target. Results shown for 100 samples, 100 validation points, and 10,000 test points.

on human-in-the-loop learning - primarily in NLP (Liu et al., 2024a) - has explored expert-guided model refinement. In time series, systems such as *DelphAI* (Kupferschmidt et al., 2022) allow manual modification of model outputs and (Arvan et al., 2019) provide a comprehensive review of human input in forecasting.

Our approach advances this line of work in two key ways. First, it enables automatic post-training corrections via adaptive optimization using reinforcement learning, bandits, or genetic algorithms. Secondly, it optionally incorporates expert feedback through natural language, automatically translated into optimization actions by a large-language model (LLM). Unlike methods such as *TimeHF* (Qi et al., 2025), which require fine-tuning large models, our solution is model-agnostic, efficient and applies corrections at inference time.

3 METHODOLOGY

We propose a framework to improve time series forecasts through *post-training optimization*. It operates on any forecasting model, applying lightweight corrections without retraining. The system combines two components: (1) **automated prediction augmentation via dynamic optimization**, and (2) **optional human-in-the-loop feedback**. We first motivate the theoretical foundation and then describe the full pipeline.

3.1 THEORETICAL MOTIVATION FOR POST-TRAINING CORRECTION

Forecasting models often display systematic biases. These can be mitigated after training by applying affine transformations to outputs, leaving model parameters unchanged. For predictions Y_{pred} , the corrected forecast is

$$Y_{\text{corrected}} = a^* Y_{\text{pred}} + b^*,$$

with optimal parameters from validation statistics:

$$a^* = \frac{\text{Cov}(Y_{\text{true}}, Y_{\text{pred}})}{\text{Var}(Y_{\text{pred}})}, \quad b^* = \mathbb{E}[Y_{\text{true}}] - a^* \mathbb{E}[Y_{\text{pred}}].$$

Theorem 1 (Affine Correction Reduces MSE) *The above correction guarantees a lower or equal mean squared error (MSE):*

$$R_{\text{before}} - R_{\text{after}} = \left(\sqrt{\text{Var}(Y_{\text{pred}})} - \frac{\text{Cov}(Y_{\text{true}}, Y_{\text{pred}})}{\sqrt{\text{Var}(Y_{\text{pred}})}} \right)^2 \geq 0.$$

This result holds under distributional alignment of validation and test sets. Figure 3 shows the mean squared error as a function of the ridge regularization parameter for a ridge regression model with an added linear post-layer correction, illustrating the result of Theorem 1. Although affine post-hoc adjustments are effective, multi-step forecasts often require richer, dynamic corrections optimized via reinforcement learning, contextual bandits, or genetic algorithms (see Section 3.3).

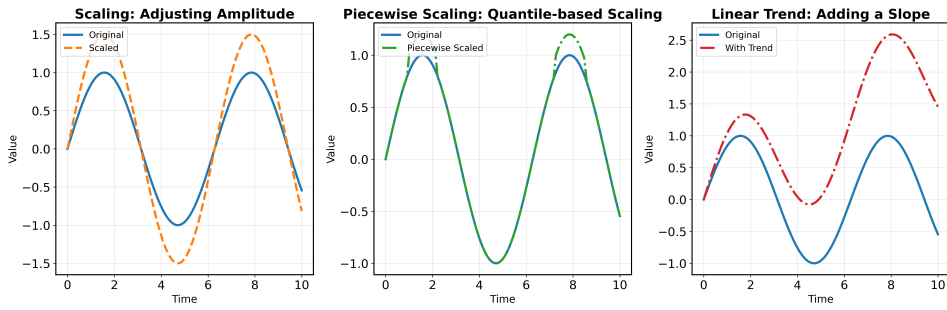
162 3.2 FORECASTING MODEL SETUP
 163

164 The framework is model-agnostic: it applies to classical (e.g., ARIMA, Prophet), deep learning (e.g.,
 165 LSTM, Transformer), and foundation models (e.g., TimesFM, Chronos). Given a multivariate time
 166 series, of length T , $\{\mathbf{x}_1, \dots, \mathbf{x}_T\}$ with $\mathbf{x}_t \in \mathbb{R}^d$, the base model outputs $\{\hat{\mathbf{y}}_{T+1}, \dots, \hat{\mathbf{y}}_{T+H}\}$, which
 167 are refined post-training. Our objective is to design a post-training method that takes the output of the
 168 base model and produces corrected predictions, improving accuracy and generalization.

169
 170 3.3 POST-TRAINING OPTIMIZATION VIA ACTION SPACE
 171

172 To refine model predictions, we define a set of post-training transformations, or *actions*, each
 173 parameterized continuously. These actions are dynamically selected and tuned to minimize validation
 174 error.

175
 176 • **Scale Amplitude:** Multiplies the full prediction series.
 177 • **Piecewise Scaling:** Modifies high or low quantiles selectively.
 178 • **Linear Trend:** Adds a slope or intercept term.
 179 • **Min/Max Adjustment:** Boosts extrema to match observed dynamics.



191
 192 Figure 4: Examples of learned post-training actions. Each transformation operates on the model’s
 193 forecast to reduce prediction error. Full action definitions are in Appendix A.1.

194
 195 These interpretable actions form a flexible augmentation layer. They can be optimized efficiently and
 196 extended to task-specific needs, as discussed in later sections.

197
 198 3.3.1 OPTIMIZING ACTIONS AND PARAMETERS

199
 200 We frame the post-training refinement process as a joint optimization over a discrete set of actions
 201 and their associated continuous parameters. Discrete actions (e.g., scaling, shifting, trend) define
 202 transformation types, while parameters control their magnitude. The goal is to select and tune the
 203 best combination to minimize validation loss.

204 **Algorithm 1:** Forecast Augmentation via Post-Training Optimization

205 **Input:** Forecasting model \mathcal{M} , action space \mathcal{A} , validation data D
 206 **Output:** Augmented model \mathcal{M}_{opt} , refined prediction $\hat{\mathbf{y}}$

207 1 Generate base predictions $\hat{\mathbf{y}} = \mathcal{M}(D)$
 208 2 Define the **loss function** $\bar{\mathcal{L}}$ (e.g., MSE) on validation set
 209 3 **for each iteration do**
 210 4 Select candidate action(s) from \mathcal{A}
 211 5 Optimize associated parameters (e.g., line search)
 212 6 Apply transformation(s) to $\hat{\mathbf{y}}$
 213 7 Evaluate $\bar{\mathcal{L}}$ and update strategy
 214 8 Return best transformation sequence

216 3.3.2 DYNAMIC OPTIMIZATION STRATEGIES
217

218 We explore several strategies to solve this search problem efficiently:
219

220 • **Random search:** For each discrete action, we randomly generate several sets of continuous
221 parameters. We then evaluate these and keep the set that gives the best performance for that
222 action.

223 • **Bandit Algorithms (SH-HPO):** (Karnin et al., 2013) Each action is a bandit arm; its
224 parameters are optimized independently (e.g., via line search). UCB balances exploration
225 and exploitation to select the most rewarding transformations.

226 • **Reinforcement Learning (PPO):** (Schulman et al., 2017) Discretizing the parameter space
227 allows us to train an RL agent that sequentially selects actions to minimize residual error.
228 We use Proximal Policy Optimization (PPO) for stability.

229 • **Genetic Algorithms (GA):** (Holland, 1975) GA evolves action-parameter pairs through
230 mutation and crossover, well-suited for large, multimodal spaces where gradients are un-
231 available or unreliable.
232

233 These techniques provide trade-offs between exploration depth and runtime. Our framework supports
234 all three and can switch strategies based on task complexity.
235

236 3.3.3 WHY DISCRETE ACTIONS + CONTINUOUS PARAMETERS
237

238 The hybrid search space balances flexibility, efficiency, and interpretability without altering the base
239 model. Advantages include: (i) reduced search complexity, (ii) human-readable corrections, (iii)
240 faster convergence, and (iv) extensibility to new domains. To mitigate overfitting, we first evaluate
241 actions on a validation set and then verify that they also improve performance on the training set.
242 This "consistency check" helps ensure that selected actions yield genuine, generalizable gains rather
243 than overfitting to the validation set. Empirically, we find that overfitting is rare in our experiments:
244 cross-metric experiments in Appendix A.5 show strong agreement between training, validation, and
245 test landscapes across different metrics throughout the episodes.
246

247 3.4 OPTIMIZATION STRATEGY: EMPIRICAL COMPARISON
248

249 We compare Random Search, SH-HPO (Successive Halving with UCB), Proximal Policy Optimiza-
250 tion (PPO), and Genetic Algorithms (GA) on the ETTH1 dataset. All methods improve over the
251 baseline, with SH-HPO giving the most consistent gains across horizons. Random Search also
252 performs strongly, often matching SH-HPO while being simpler and more efficient. Their advantage
253 likely stems from naturally handling discrete-continuous search spaces, whereas PPO and GA require
254 full discretization, which increases complexity and introduces approximation errors that reduce
255 effectiveness. Nevertheless, PPO and GA remain valuable for tasks needing long-term optimization,
256 since they explore trajectories rather than making greedy, step-wise decisions. Despite lower per-
257 formance here, they may be better suited to structured or sequential problems. For the remainder of our
258 experiments, we adopt Random Search for its simplicity, efficiency, and competitive results. Full
259 results and additional dataset comparisons are in the Appendix.
260

261 **Evaluation Metric for Post-Training.** To assess post-training effectiveness, we use the relative
262 decrease in mean squared error (MSE). Let MSE_{before} and MSE_{after} denote the model's MSE before
263 and after post-training. The relative improvement is
264

$$\mathcal{M} = \frac{MSE_{\text{before}} - MSE_{\text{after}}}{MSE_{\text{before}}}. \quad (1)$$

265 Positive \mathcal{M} indicates reduced error, higher values reflect greater improvement, and negative \mathcal{M}
266 indicates post-training degraded performance. This normalized metric enables fair comparison across
267 models and datasets with different MSE scales. Complementary experiments using other metrics are
268 reported in Appendix A.5.
269

Table 1: Performance comparison of different optimization techniques. Reported values are percentage improvements in mean squared error (MSE) relative to baseline models, averaged over 10 trials on the **Nature** dataset. Standard deviations are shown as uncertainty.

Model	Random	SH-HPO	RL (PPO)	GA
AutoFormer	$17.19\% \pm 5.3\%$	$19.34\% \pm 5.1\%$	$3.35\% \pm 1.2\%$	$6.09\% \pm 1.5\%$
Crossformer	$3.30\% \pm 2.1\%$	$2.78\% \pm 1.9\%$	$1.11\% \pm 1.4\%$	$1.52\% \pm 1.3\%$
DLinear	$1.96\% \pm 0.8\%$	$1.57\% \pm 0.7\%$	$2.20\% \pm 1.1\%$	$1.61\% \pm 0.9\%$
PatchTST	$-1.33\% \pm 1.2\%$	$-0.81\% \pm 1.0\%$	$0.26\% \pm 0.5\%$	$0.29\% \pm 0.4\%$
SegRNN	$1.70\% \pm 0.6\%$	$2.59\% \pm 0.8\%$	$0.61\% \pm 0.4\%$	$0.59\% \pm 0.5\%$
iTransformer	$3.10\% \pm 1.1\%$	$3.85\% \pm 1.3\%$	$1.33\% \pm 0.7\%$	$1.50\% \pm 0.8\%$
TimesFM	$4.94\% \pm 2.3\%$	$5.43\% \pm 2.1\%$	$3.48\% \pm 1.5\%$	$2.62\% \pm 1.4\%$
Average	$4.84\% \pm 1.9\%$	$4.96\% \pm 1.9\%$	$1.76\% \pm 1.1\%$	$2.32\% \pm 1.3\%$

4 THEORETICAL ANALYSIS OF OUR BANDIT-BASED CORRECTION

Our method evaluates a large set of corrective actions (Section 3.3) and selects the best one using several candidate selection strategies. Among them, the bandit-based approach with the *Successive Halving* algorithm consistently achieves the strongest results in our experiments.

Natural questions are: *how quickly does this algorithm identify the best correction?* and *How does the validation budget affect its performance?* This section answers those questions theoretically. We focus on the simplest non-trivial setting of two corrective actions to present the key result; the general case ($K > 2$ actions) and all proofs are deferred to Appendix A.

Why Successive Halving. Successive Halving is a near-optimal best-arm identification algorithm (Karnin et al., 2013). It allocates more evaluations to promising actions while discarding the worse ones. This matches our setting, where evaluating each correction on the validation set is costly, and explains its superior empirical performance compared to uniform allocation.

Corollary 1 (Convergence to the Best Correction) Consider two corrective actions g_{1,β^*} and g_{2,β^*} with $R(g_{1,\beta^*} \circ f_\theta) < R(g_{2,\beta^*} \circ f_\theta)$ and a validation budget of T evaluations. Under Assumption 1 (Appendix A.11), the correction selected by our bandit-based procedure satisfies:

$$\mathbb{E}[R(g_{k_T, \beta^*} \circ f_\theta)] \leq 2R(g_{1, \beta^*} \circ f_\theta) + 2\Delta \Phi(-\Delta\sqrt{T}), \quad \Delta = R(g_{2, \beta^*} \circ f_\theta) - R(g_{1, \beta^*} \circ f_\theta),$$

where Φ is the standard Gaussian CDF.

This bound shows that the expected risk of the selected correction converges exponentially fast in \sqrt{T} to the risk of the best correction. Larger risk gaps Δ (i.e. more distinct corrective actions) lead to faster convergence.

Corollary 2 (Budget to Outperform the Base Model) *To guarantee that the selected correction improves on f_θ , it suffices to allocate T evaluations, with*

$$T \gtrsim \frac{4}{\Delta^2} \left[\Phi^{-1} \left(\frac{R(f_\theta) - 2R(g_{1,\beta^*} \circ f_\theta)}{2\Delta} \right) \right]^2.$$

These results directly explain our empirical findings (Table 6): with a reasonable validation budget and sufficiently distinct corrective actions, the Successive Halving algorithm quickly identifies the best correction and improves forecasting accuracy. The general case and all proofs appear in Appendix A 11.

324 5 HUMAN-IN-THE-LOOP FEEDBACK INTEGRATION

325

326 Our framework operates autonomously but supports optional human-in-the-loop (HITL) refinement.
327 Domain experts can provide natural language suggestions (e.g., *“Increase values above the 80th*
328 *percentile”*), which are translated into candidate actions via an LLM (e.g., Qwen2-72B-32K).
329 Crucially, human feedback never directly modifies predictions; instead, it must pass through the same
330 optimization and validation pipeline as automated actions, ensuring safety and performance.

331
332 **From Natural Language to Candidate Actions** User prompts are converted into executable
333 Python code and added to the candidate pool only after validation (Algorithm 2, Figure 5). If the
334 initial suggestion fails, users can refine their input iteratively.

335 **Algorithm 2:** Human-in-the-Loop Feedback Integration

336 **Input:** User prompt p
337 1 **while** $true$ **do**
338 2 $a \leftarrow \text{LLM}(p)$
339 3 **if** $\text{Test}(a)$ **then**
340 4 $\text{AddActionToPool}(a)$
341 5 **break**
342 6 $p \leftarrow \text{RequestNewPrompt}()$

344 **Provide Feedback**

345 Enter your feedback for the model’s predictions
346
347 The amplitude of the predictions should be increased between 5% and 10% of the actual value.
348 Press Ctrl+Enter to apply
349
350 Select the channel to provide feedback for
351 0
352

353 (a) User input prompt

```
354 class GenericFunction:  
355     def __init__(self, function_type, params):  
356         self.function_type = function_type  
357         self.params = params  
358  
359     def apply(self, prediction, batch_x):  
360         if self.function_type == 'increase_amplitude':  
361             increase_percentage = self.params['increase_percentage']  
362             return prediction * (1 + increase_percentage / 100)  
363         # Add more conditions for other function_types if needed  
364         else:  
365             raise ValueError("Unknown function_type: " + self.function_type)  
366  
367     def generate_random_params_for_action(self, action, batch_x):  
368         if action == 'increase_amplitude':  
369             # Assuming the increase percentage is randomly chosen between 5% and 10%  
370             import random  
371             return {'increase_percentage': random.uniform(5, 10)}  
372             # Add more conditions for other actions if needed  
373         else:  
374             raise ValueError("Unknown action: " + action)
```

355 (b) Generated code for adaptive optimization

356 Figure 5: HITL pipeline: prompts are converted to code and validated before entering the candidate
357 pool.

358 **Interactive Refinement and Safety** Users can iteratively refine prompts to improve candidate
359 quality. All proposed actions undergo strict validation ($\text{Test}()$) for API compliance, execution, and
360 forecast validity. The LLM never accesses raw time series data, preventing leakage or overfitting.

361
362 **Integration with Optimization** Validated human-proposed actions are evaluated alongside auto-
363 mated candidates in the optimization loop (Section 3.3). Only actions that improve performance are
364 retained, ensuring robustness. Case studies in Section A.6.1 demonstrate this mechanism in practice.

365 6 EXPERIMENTS

366 We evaluate our framework across diverse real-world time series tasks, demonstrating consistent
367 improvements in forecast accuracy using standard benchmarks and open-source implementations. All
368 experiments were conducted on a server equipped with 2x Intel Xeon E5-2690 v4 CPUs (56 cores
369 total), 512 GB RAM, and 6x NVIDIA Tesla P100 GPUs (16 GB each), though only one GPU was
370 used per run.

371 6.1 SETUP

372 We evaluate our post-training optimization framework on energy consumption and OpenTS bench-
373 mark datasets (Zhou et al., 2021; Qiu et al., 2024) (details in Appendix A.2.1), across a wide range of
374 forecasting models—from simple deep learning models such as DLinear (Zeng et al., 2023) to modern

378 architectures including SegRNN (Lin et al., 2023), iTransformer (Liu et al., 2023), PatchTST (Nie
379 et al., 2023), Autoformer (Wu et al., 2021), Crossformer (Zhang & Yan, 2023), and Informer (Zhou
380 et al., 2021). Forecast accuracy is reported using Mean Squared Error (MSE), averaged across
381 multiple horizons (96, 192, 336, 720). Although performance is measured in MSE, our model-
382 agnostic framework is compatible with any optimization or evaluation metric (e.g., MAE, MAPE,
383 R^2); Section A.5 presents complementary experiments confirming its robustness and showing that it
384 mitigates overfitting to the validation set.

385 While our framework can work with training samples alone, it generally requires for better perfor-
386 mance a representative validation set for time series forecasting, in line with established practices. For
387 benchmark datasets like ETTh1, ETTh2, ETM1, and ETM2, which provide an explicit validation
388 set (designated by a ‘val’ flag), we use these validation sets directly. For datasets without an explicit
389 validation set, we apply the standard approach of temporally splitting the training data, allocating
390 30% to the validation set. This method aligns with common practices in the field of time series
391 forecasting. We conduct a robustness analysis of the training-validation ratio in Section A.3.

392

393 6.2 RESULTS: ADAPTIVE OPTIMIZATION IMPROVES FORECASTING

394

395 Table 2 summarizes the impact of our post-training optimization. Across nearly all models and
396 datasets, we observe significant MSE reductions with no retraining and minimal overhead (and **very**
397 **few cases of overfitting in orange**). Rare cases of negative improvement can mostly be attributed
398 to the stochastic nature of the search. The search algorithm iteratively evaluates the performance of
399 actions on the validation set. As discussed in Subsection 3.3.3 and Appendix A.5, our approach is
400 not prone to overfitting to the validation set; however, as shown in Section 4, it still induces a failure
401 probability δ .

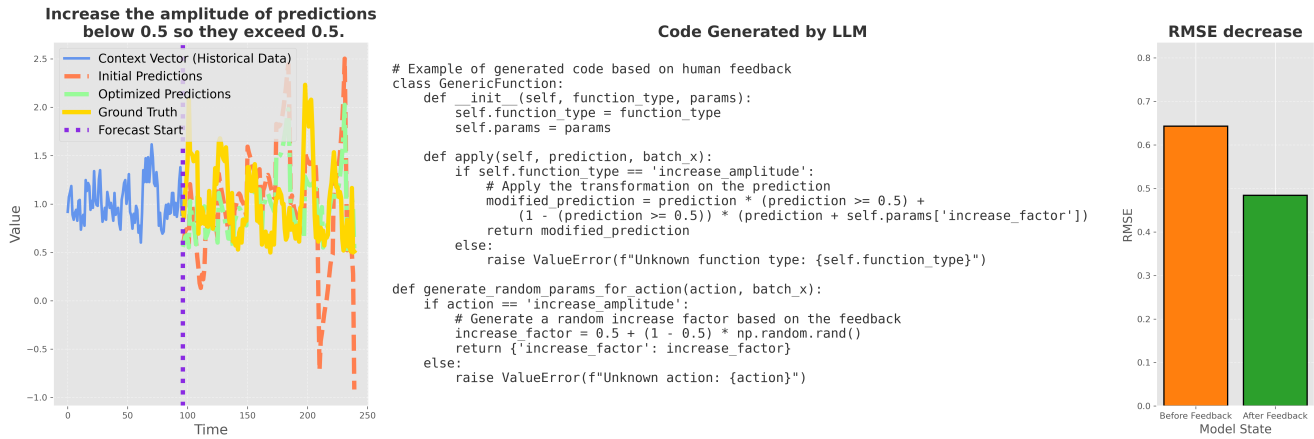
402

403 6.2.1 HUMAN-IN-THE-LOOP FEEDBACK

404

405 Human feedback can further enhance forecast accuracy by introducing domain knowledge not
406 captured by the base model. Users provide natural language instructions (e.g., “*increase the amplitude*
407 of predictions below 0.5”), which are converted into executable transformations via a large language
408 model (LLM).

409



424

425 Figure 6: (a) Initial prediction vs. human-refined forecast. (b) Action code generated from natural
426 language via LLM (Qwen2-72B-32K). (c) RMSE improvement post-feedback.

427

428 Figure 6 shows that integrating expert suggestions via HITL leads to tangible performance gains.
429 Additional examples are presented in Appendix A.6 (see Figures 13, 14 and 15). The interface
430 supports real-time experimentation, making human-guided optimization practical and intuitive. **It is**
431 **important to emphasize that the code generated by the LLM is guided by a strict template, which is**
detailed in the Appendix (Section A.6). This template constrains the possible code outputs, ensuring

Methods	Autoformer	Crossformer	iTransformer	PatchTST	DLinear	SegRNN	Informer
<i>ETTh1</i>	$0.61 \pm 0.01 \rightarrow 0.51 \pm 0.02$ (16.76%)	$0.54 \pm 0.01 \rightarrow 0.52 \pm 0.01$ (2.20%)	$0.45 \pm 0.01 \rightarrow 0.44 \pm 0.01$ (2.58%)	$0.46 \pm 0.01 \rightarrow 0.47 \pm 0.01$ (-2.25%)	$0.47 \pm 0.01 \rightarrow 0.45 \pm 0.01$ (1.38%)	$0.47 \pm 0.01 \rightarrow 0.45 \pm 0.01$ (1.31%)	$0.67 \pm 0.01 \rightarrow 0.65 \pm 0.01$ (3.00%)
<i>ETTh2</i>	$0.65 \pm 0.01 \rightarrow 0.55 \pm 0.01$ (15.48%)	$0.60 \pm 0.01 \rightarrow 0.57 \pm 0.01$ (3.7%)	$0.60 \pm 0.01 \rightarrow 0.57 \pm 0.01$ (4.0%)	$0.60 \pm 0.01 \rightarrow 0.57 \pm 0.01$ (4.2%)	$0.60 \pm 0.01 \rightarrow 0.57 \pm 0.01$ (3.8%)	$0.60 \pm 0.01 \rightarrow 0.57 \pm 0.01$ (3.8%)	$0.60 \pm 0.01 \rightarrow 0.57 \pm 0.01$ (3.9%)
<i>ETTm1</i>	$0.60 \pm 0.01 \rightarrow 0.57 \pm 0.01$ (7.37%)	$0.60 \pm 0.01 \rightarrow 0.57 \pm 0.01$ (3.7%)	$0.60 \pm 0.01 \rightarrow 0.57 \pm 0.01$ (4.0%)	$0.60 \pm 0.01 \rightarrow 0.57 \pm 0.01$ (4.2%)	$0.60 \pm 0.01 \rightarrow 0.57 \pm 0.01$ (3.8%)	$0.60 \pm 0.01 \rightarrow 0.57 \pm 0.01$ (3.8%)	$0.60 \pm 0.01 \rightarrow 0.57 \pm 0.01$ (3.9%)
<i>ETTm2</i>	$0.60 \pm 0.01 \rightarrow 0.57 \pm 0.01$ (20.25%)	$3.82 \pm 0.01 \rightarrow 3.81 \pm 0.01$ (3.7%)	$0.60 \pm 0.01 \rightarrow 0.57 \pm 0.01$ (4.0%)	$0.60 \pm 0.01 \rightarrow 0.57 \pm 0.01$ (4.2%)	$0.60 \pm 0.01 \rightarrow 0.57 \pm 0.01$ (3.8%)	$0.60 \pm 0.01 \rightarrow 0.57 \pm 0.01$ (3.8%)	$0.60 \pm 0.01 \rightarrow 0.57 \pm 0.01$ (3.9%)
<i>Dominick</i>	$1.38 \pm 0.01 \rightarrow 1.16 \pm 0.01$ (15.42%)	$1.12 \pm 0.01 \rightarrow 1.10 \pm 0.01$ (1.00%)	$1.25 \pm 0.01 \rightarrow 1.23 \pm 0.01$ (0.89%)	$1.25 \pm 0.01 \rightarrow 1.20 \pm 0.01$ (3.83%)	$1.24 \pm 0.01 \rightarrow 1.13 \pm 0.01$ (7.97%)	$1.92 \pm 0.01 \rightarrow 1.40 \pm 0.01$ (27.21%)	$1.14 \pm 0.01 \rightarrow 1.09 \pm 0.01$ (4.28%)
<i>Human</i>	$0.40 \pm 0.01 \rightarrow 0.33 \pm 0.01$ (20.24%)	$0.30 \pm 0.01 \rightarrow 0.25 \pm 0.01$ (13.34%)	$0.60 \pm 0.01 \rightarrow 0.15 \pm 0.01$ (51.26%)	$0.62 \pm 0.01 \rightarrow 0.15 \pm 0.01$ (51.74%)	$0.96 \pm 0.01 \rightarrow 0.26 \pm 0.01$ (57.85%)	$0.60 \pm 0.01 \rightarrow 0.25 \pm 0.01$ (43.02%)	$0.30 \pm 0.01 \rightarrow 0.21 \pm 0.01$ (21.93%)
<i>KDD</i>	$1.25 \pm 0.01 \rightarrow 0.95 \pm 0.01$ (23.50%)	$0.80 \pm 0.01 \rightarrow 0.80 \pm 0.01$ (-0.03%)	$1.13 \pm 0.01 \rightarrow 0.88 \pm 0.01$ (21.09%)	$1.14 \pm 0.01 \rightarrow 0.89 \pm 0.01$ (21.83%)	$0.93 \pm 0.01 \rightarrow 0.85 \pm 0.01$ (8.54%)	$1.10 \pm 0.01 \rightarrow 0.88 \pm 0.01$ (19.14%)	$1.12 \pm 0.01 \rightarrow 0.87 \pm 0.01$ (22.15%)
<i>Nature</i>	$1.25 \pm 0.01 \rightarrow 0.96 \pm 0.01$ (21.69%)	$0.65 \pm 0.01 \rightarrow 0.66 \pm 0.01$ (-1.17%)	$0.34 \pm 0.01 \rightarrow 0.33 \pm 0.01$ (3.26%)	$0.26 \pm 0.01 \rightarrow 0.25 \pm 0.01$ (3.72%)	$0.95 \pm 0.01 \rightarrow 0.91 \pm 0.01$ (4.31%)	$1.02 \pm 0.01 \rightarrow 0.94 \pm 0.01$ (8.67%)	$0.91 \pm 0.01 \rightarrow 0.90 \pm 0.01$ (0.86%)
<i>NASDAQ</i>	$0.91 \pm 0.01 \rightarrow 0.70 \pm 0.01$ (22.39%)	$0.46 \pm 0.01 \rightarrow 0.46 \pm 0.01$ (-0.33%)	$0.80 \pm 0.01 \rightarrow 0.63 \pm 0.01$ (19.77%)	$0.79 \pm 0.01 \rightarrow 0.68 \pm 0.01$ (14.76%)	$0.74 \pm 0.01 \rightarrow 0.68 \pm 0.01$ (7.59%)	$0.78 \pm 0.01 \rightarrow 0.62 \pm 0.01$ (19.19%)	$0.85 \pm 0.01 \rightarrow 0.79 \pm 0.01$ (8.96%)
<i>Pedestrian</i>	$0.46 \pm 0.01 \rightarrow 0.27 \pm 0.01$ (40.01%)	$0.14 \pm 0.01 \rightarrow 0.13 \pm 0.01$ (0.26%)	$0.14 \pm 0.01 \rightarrow 0.12 \pm 0.01$ (9.43%)	$0.22 \pm 0.01 \rightarrow 0.19 \pm 0.01$ (9.54%)	$0.69 \pm 0.01 \rightarrow 0.60 \pm 0.01$ (14.20%)	$0.20 \pm 0.01 \rightarrow 0.18 \pm 0.01$ (6.94%)	$0.33 \pm 0.01 \rightarrow 0.27 \pm 0.01$ (15.87%)
<i>Tourism</i>	$0.24 \pm 0.01 \rightarrow 0.22 \pm 0.01$ (10.88%)	$0.16 \pm 0.01 \rightarrow 0.14 \pm 0.01$ (11.48%)	$0.31 \pm 0.01 \rightarrow 0.14 \pm 0.01$ (40.08%)	$0.31 \pm 0.01 \rightarrow 0.14 \pm 0.01$ (39.20%)	$0.52 \pm 0.01 \rightarrow 0.25 \pm 0.01$ (48.91%)	$0.24 \pm 0.01 \rightarrow 0.12 \pm 0.01$ (48.14%)	$0.22 \pm 0.01 \rightarrow 0.18 \pm 0.01$ (20.57%)
<i>Vehicle trips</i>	$1.39 \pm 0.01 \rightarrow 1.13 \pm 0.01$ (18.13%)	$0.83 \pm 0.01 \rightarrow 0.82 \pm 0.01$ (0.89%)	$1.02 \pm 0.01 \rightarrow 0.84 \pm 0.01$ (17.14%)	$0.98 \pm 0.01 \rightarrow 0.80 \pm 0.01$ (18.00%)	$1.35 \pm 0.01 \rightarrow 1.15 \pm 0.01$ (14.37%)	$1.68 \pm 0.01 \rightarrow 1.05 \pm 0.01$ (38.46%)	$1.21 \pm 0.01 \rightarrow 0.95 \pm 0.01$ (21.54%)

Table 2: Mean squared error (MSE) \pm standard deviation across multiple forecast horizons, before and after applying Adaptive Optimization (\rightarrow). Improvements are reported in **teal** when positive and **orange** when negative. The overall improvement across all models and datasets is 14.84%, with a peak improvement of 57.85%. This is based on 12 datasets and 7 time series models, with only 4 cases (out of 84) showing a performance decline, averaging -0.94% and a maximum of -2.25%.

that only valid and meaningful actions are generated. Additionally, the LLM not only generates the transformation code but also a function that creates a pool of candidate parameters. These parameters are then subject to optimization (as described in details in the automated optimization framework), with ineffective candidates being discarded if they do not improve the model's performance.

To assess the robustness of the framework, we provide several failure cases where the user's prompt is ambiguous or nonsensical. We investigate three cases in Figure 16, 17 and 18 with the prompt given in the title (e.g., *Optimize model to make it model like* and *being unoptimized*, *Replace everything by random noise* and *Taratata las palsma reality bonneur selar*). In these cases, the system either discards the resulting action (if it does not lead to improvements) or the generated code fails to execute properly (improvement being 0%). These scenarios demonstrate the framework's ability to handle poor feedback and ensure that only actions leading to performance enhancement are retained.

The corresponding code generated by the LLM in these failure cases, along with additional examples, is provided in Appendix A.6.

Remark 1 (On the safety of the human-in-the-loop framework) *In addition to the automated optimization procedures, we provide an optional "safe mode". This mode displays the Python source code of the proposed actions for manual inspection by the user. The code is then automatically scanned using the malicious-source-code detector of Tsafaty & Fire (2023) before execution. This*

486 *detection step incurs only a small overhead, since each newly generated action is analyzed once at*
487 *creation time, rather than at every inference step, and the corresponding code snippets are short.*

488

489 6.2.2 COMPUTATIONAL EFFICIENCY AND SCALABILITY

490

491 We evaluate optimization time across varying forecast horizons and action space sizes on the *ETTh1*
492 dataset. Table 8 compares our post-training augmentation time against the minimum and maximum
493 training times of standard forecasting models.

494 Table 3: Adaptive optimization time vs. base model training time (10 epochs).

495

496 Horizon	497 2 Actions	498 4 Actions	499 7 Actions	500 DLinear (min)	501 PatchTST (max)
498 96	499 $3.2s \pm 0.1$	500 $5.4s \pm 0.2$	501 $12.0s \pm 1.3$	502 20.3s	503 144.4s
498 192	499 $6.1s \pm 0.3$	500 $9.7s \pm 0.4$	501 $22.7s \pm 1.5$	502 22.3s	503 146.2s
498 336	499 $12.7s \pm 0.5$	500 $18.3s \pm 0.6$	501 $30.1s \pm 1.0$	502 24.4s	503 148.8s
498 720	499 $24.3s \pm 1.1$	500 $35.2s \pm 1.4$	501 $45.1s \pm 1.8$	502 27.3s	503 151.8s

502 Even for long horizons and expanded action spaces, our optimization time remains well below the
503 training cost of most models, confirming the framework’s suitability for real-time applications and
504 large-scale deployment.

505

506 7 CONCLUSION

507

508 We presented a model-agnostic framework for time series forecasting that enhances predictions
509 through post-training optimization and optional human-in-the-loop refinement. Unlike retraining-
510 based methods, our approach applies lightweight, interpretable transformations, yielding consistent
511 accuracy gains across diverse models and datasets at low cost. The framework is broadly compatible,
512 fast, and interpretable, allowing for seamless integration of natural language feedback through LLMs.
513 Its effectiveness depends on the quality of the base model, and LLM-based feedback translation
514 may vary with prompt clarity; robustness to ambiguous instructions and access to a representative
515 validation set remain open challenges.

516 Future work includes richer transformations (e.g. monotone, piecewise-affine, uncertainty-aware),
517 stronger LLM alignment via structured prompting and automatic tests/guardrails, and applications to
518 multimodal and streaming time series with online updates and drift handling.

519
520
521
522
523
524
525
526
527
528
529
530
531
532
533
534
535
536
537
538
539

540 **REPRODUCIBILITY STATEMENT**
541

542 We detail the complete methodology and experimental settings in [section 3](#) and [section 6](#), with
543 theoretical assumptions and results in [section 4](#) and proofs in [subsubsection A.10.3](#). The action space,
544 search strategies, additional analyzes, datasets, preprocessing, splits, and model configurations appear
545 in the main paper and are detailed in the beginning of the appendix. We provide an interactive demo
546 to reproduce and test our approach. The hardware details for our runs are reported in [section 6](#). To
547 ease verification, we include: (i) fixed seeds, (ii) YAML configs for hyper-parameters, (iii) a single
548 entry-point script for each experiment, and (iv) checks that validate data splits and metrics.

549

550 **LLM USAGE STATEMENT**
551

552 We used large language models *solely for language editing* (grammar and clarity). An LLM did not
553 generate technical claims, equations, algorithms, hyperparameters, or experimental decisions. All
554 content was verified by the authors. We disclose this limited use here and in the submission form.

555

556

557

558

559

560

561

562

563

564

565

566

567

568

569

570

571

572

573

574

575

576

577

578

579

580

581

582

583

584

585

586

587

588

589

590

591

592

593

594 REFERENCES

595

596 Abdul Fatir Ansari, Lorenzo Stella, Caner Turkmen, Xiyuan Zhang, Pedro Mercado, Huibin Shen,
597 Oleksandr Shchur, Syama Sundar Rangapuram, Sebastian Pineda Arango, Shubham Kapoor, et al.
598 Chronos: Learning the language of time series. *arXiv preprint arXiv:2403.07815*, 2024.

599 J Scott Armstrong. The ombudsman: research on forecasting: A quarter-century review, 1960–1984.
600 *Interfaces*, 16(1):89–109, 1986.

601 Meysam Arvan, Behnam Fahimnia, Mohsen Reisi, and Enno Siemsen. Integrating human judgement
602 into quantitative forecasting methods: A review. *Omega*, 86:237–252, 2019.

603

604 Derek Bunn and George Wright. Interaction of judgemental and statistical forecasting methods:
605 issues & analysis. *Management science*, 37(5):501–518, 1991.

606 Abhimanyu Das, Weihao Kong, Rajat Sen, and Yichen Zhou. A decoder-only foundation model for
607 time-series forecasting. In *Forty-first International Conference on Machine Learning*, 2024.

608

609 Everette S Gardner Jr. Exponential smoothing: The state of the art. *Journal of forecasting*, 4(1):1–28,
610 1985.

611 John Geweke and Charles Whiteman. Bayesian forecasting. *Handbook of economic forecasting*, 1:
612 3–80, 2006.

613

614 Agathe Girard, Carl Rasmussen, Joaquin Q Candela, and Roderick Murray-Smith. Gaussian process
615 priors with uncertain inputs application to multiple-step ahead time series forecasting. *Advances in
616 neural information processing systems*, 15, 2002.

617 Alex Graves and Alex Graves. Long short-term memory. *Supervised sequence labelling with
618 recurrent neural networks*, pp. 37–45, 2012.

619

620 John H. Holland. *Adaptation in Natural and Artificial Systems*. University of Michigan Press, Ann
621 Arbor, MI, 1975.

622 Romain Ilbert, Ambroise Odonnat, Vasilii Feofanov, Aladin Virmaux, Giuseppe Paolo, Themis
623 Palpanas, and Ievgen Redko. Samformer: Unlocking the potential of transformers in time se-
624 ries forecasting with sharpness-aware minimization and channel-wise attention. *arXiv preprint
625 arXiv:2402.10198*, 2024.

626

627 Zohar S. Karnin, Tomer Koren, and Oren Somekh. Almost optimal exploration in multi-armed bandits.
628 In *Proceedings of the 30th International Conference on Machine Learning*, pp. 1238–1246. PMLR,
629 2013.

630 Shruti Kaushik, Abhinav Choudhury, Pankaj Kumar Sheron, Nataraj Dasgupta, Sayee Natarajan,
631 Larry A Pickett, and Varun Dutt. Ai in healthcare: time-series forecasting using statistical, neural,
632 and ensemble architectures. *Frontiers in big data*, 3:4, 2020.

633 Mehdi Khashei and Mehdi Bijari. A new class of hybrid models for time series forecasting. *Expert
634 Systems with Applications*, 39(4):4344–4357, 2012.

635

636 Joos Korstanje. The sarima model. In *Advanced Forecasting with Python: With State-of-the-Art-
637 Models Including LSTMs, Facebook’s Prophet, and Amazon’s DeepAR*, pp. 115–122. Springer,
638 2021.

639 Bjoern Krollner, Bruce Vanstone, and Gavin Finnie. Financial time series forecasting with ma-
640 chine learning techniques: A survey. In *European Symposium on Artificial Neural Networks:
641 Computational Intelligence and Machine Learning*, pp. 25–30, 2010.

642 Kristina L Kupferschmidt, Joshua G Skorburg, and Graham W Taylor. Delphai: A human-centered
643 approach to time-series forecasting. In *2022 IEEE International Conference on Big Data (Big
644 Data)*, pp. 4014–4020. IEEE, 2022.

645

646 Shengsheng Lin, Weiwei Lin, Wentai Wu, Feiyu Zhao, Ruichao Mo, and Haotong Zhang. Seg-
647 rnn: Segment recurrent neural network for long-term time series forecasting. *arXiv preprint
arXiv:2308.11200*, 2023.

648 Aixin Liu, Bei Feng, Bing Xue, Bingxuan Wang, Bochao Wu, Chengda Lu, Chenggang Zhao,
649 Chengqi Deng, Chenyu Zhang, Chong Ruan, et al. Deepseek-v3 technical report. *arXiv preprint*
650 *arXiv:2412.19437*, 2024a.

651 Haoxin Liu, Shangqing Xu, Zhiyuan Zhao, Lingkai Kong, Harshavardhan Kamarthi, Aditya B
652 Sasanur, Megha Sharma, Jiaming Cui, Qingsong Wen, Chao Zhang, et al. Time-mmd: A new
653 multi-domain multimodal dataset for time series analysis. *arXiv preprint arXiv:2406.08627*, 2024b.

654 Yong Liu, Tengge Hu, Haoran Zhang, Haixu Wu, Shiyu Wang, Lintao Ma, and Mingsheng Long.
655 itransformer: Inverted transformers are effective for time series forecasting. *arXiv preprint*
656 *arXiv:2310.06625*, 2023.

657 Shahrbanou Madadgar, Hamid Moradkhani, and David Garen. Towards improved post-processing of
658 hydrologic forecast ensembles. *Hydrological Processes*, 28(1):104–122, 2014.

659 Stefan Meisenbacher, Marian Turowski, Kaleb Phipps, Martin Rätz, Dirk Müller, Veit Hagenmeyer,
660 and Ralf Mikut. Review of automated time series forecasting pipelines. *Wiley Interdisciplinary*
661 *Reviews: Data Mining and Knowledge Discovery*, 12(6):e1475, 2022.

662 Paul Newbold. Arima model building and the time series analysis approach to forecasting. *Journal*
663 *of forecasting*, 2(1):23–35, 1983.

664 Yuqi Nie, Nam H. Nguyen, Phanwadee Sinthong, and Jayant Kalagnanam. A time series is worth
665 64 words: Long-term forecasting with transformers. In *International Conference on Learning*
666 *Representations*, 2023.

667 Giulia Palma, Elna Sara Joy Chengalipunath, and Antonio Rizzo. Time series forecasting for
668 energy management: Neural circuit policies (ncps) vs. long short-term memory (lstm) networks.
669 *Electronics*, 13(18):3641, 2024.

670 Yongzhi Qi, Hao Hu, Dazhou Lei, Jianshen Zhang, Zhengxin Shi, Yulin Huang, Zhengyu Chen,
671 Xiaoming Lin, and Zuo-Jun Max Shen. Timehf: Billion-scale time series models guided by human
672 feedback. *arXiv preprint arXiv:2501.15942*, 2025.

673 Xiangfei Qiu, Jilin Hu, Lekui Zhou, Xingjian Wu, Junyang Du, Buang Zhang, Chenjuan Guo, Aoying
674 Zhou, Christian S Jensen, Zhenli Sheng, and Bin Yang. Tfb: Towards comprehensive and fair
675 benchmarking of time series forecasting methods. *Proc. VLDB Endow.*, 17:2363 – 2377, 2024.

676 Kashif Rasul, Arjun Ashok, Andrew Robert Williams, Hena Ghonia, Rishika Bhagwatkar, Arian
677 Khorasani, Mohammad Javad Darvishi Bayazi, George Adamopoulos, Roland Riachi, Nadhir
678 Hassen, et al. Lag-llama: Towards foundation models for probabilistic time series forecasting.
679 *arXiv preprint arXiv:2310.08278*, 2023.

680 Jeffrey R Sampson. Adaptation in natural and artificial systems (john h. holland), 1976.

681 John Schulman, Filip Wolski, Prafulla Dhariwal, Alec Radford, and Oleg Klimov. Proximal policy
682 optimization algorithms. *arXiv preprint arXiv:1707.06347*, 2017.

683 Romain Tavenard, Johann Faouzi, Gilles Vandewiele, Felix Divo, Guillaume Androz, Chester Holtz,
684 Marie Payne, Roman Yurchak, Marc Rußwurm, Kushal Kolar, et al. Tslearn, a machine learning
685 toolkit for time series data. *Journal of machine learning research*, 21(118):1–6, 2020.

686 Chen Tsafaty and Michael Fire. Malicious source code detection using a translation model. *Patterns*,
687 4(7), 2023.

688 JS Verkade, JD Brown, P Reggiani, and AH Weerts. Post-processing ecmwf precipitation and
689 temperature ensemble reforecasts for operational hydrologic forecasting at various spatial scales.
690 *Journal of Hydrology*, 501:73–91, 2013.

691 Richard Webby and Marcus O'Connor. Judgemental and statistical time series forecasting: a review
692 of the literature. *International Journal of forecasting*, 12(1):91–118, 1996.

693 Haixu Wu, Jiehui Xu, Jianmin Wang, and Mingsheng Long. Autoformer: Decomposition transformers
694 with auto-correlation for long-term series forecasting. *Advances in neural information processing*
695 *systems*, 34:22419–22430, 2021.

702 Ailing Zeng, Muxi Chen, Lei Zhang, and Qiang Xu. Are transformers effective for time series
703 forecasting? In *Proceedings of the AAAI conference on artificial intelligence*, volume 37, pp.
704 11121–11128, 2023.

705 Yunhao Zhang and Junchi Yan. Crossformer: Transformer utilizing cross-dimension dependency
706 for multivariate time series forecasting. In *The eleventh international conference on learning
707 representations*, 2023.

708 Haoyi Zhou, Shanghang Zhang, Jieqi Peng, Shuai Zhang, Jianxin Li, Hui Xiong, and Wancai Zhang.
709 Informer: Beyond efficient transformer for long sequence time-series forecasting. In *Proceedings
710 of the AAAI conference on artificial intelligence*, volume 35, pp. 11106–11115, 2021.

711 Yanlai Zhou. Real-time probabilistic forecasting of river water quality under data missing situation:
712 Deep learning plus post-processing techniques. *Journal of Hydrology*, 589:125164, 2020.

713
714
715
716
717
718
719
720
721
722
723
724
725
726
727
728
729
730
731
732
733
734
735
736
737
738
739
740
741
742
743
744
745
746
747
748
749
750
751
752
753
754
755

756	A APPENDIX	
757		
758		
759	TABLE OF CONTENTS	
760		
761	1 Introduction	1
762		
763	2 Related Work	2
764		
765		
766	3 Methodology	3
767	3.1 Theoretical Motivation for Post-Training Correction	3
768		
769	3.2 Forecasting Model Setup	4
770	3.3 Post-Training Optimization via Action Space	4
771	3.3.1 Optimizing Actions and Parameters	4
772	3.3.2 Dynamic Optimization Strategies	5
773	3.3.3 Why Discrete Actions + Continuous Parameters	5
774	3.4 Optimization Strategy: Empirical Comparison	5
775		
776		
777		
778	4 Theoretical Analysis of Our Bandit-Based Correction	6
779		
780		
781	5 Human-in-the-Loop Feedback Integration	7
782		
783	6 Experiments	7
784	6.1 Setup	7
785		
786	6.2 Results: Adaptive Optimization Improves Forecasting	8
787	6.2.1 Human-in-the-Loop Feedback	8
788	6.2.2 Computational Efficiency and Scalability	10
789		
790		
791	7 Conclusion	10
792		
793		
794	A Appendix	15
795	A.1 Mathematical definitions and visualizations of the pool of actions	16
796		
797	A.2 Details on experimental setup: Datasets and models	17
798	A.3 More experiments on the reinforcement automated loop	18
799		
800	A.4 Experiments on Performance Improvement as a Function of the Number of Actions	25
801		
802	A.5 Cross-Metric Evaluation of Optimization Strategies	26
803		
804	A.6 More experiments on the human feedback	26
805		
806	A.7 Code and Reproducibility	31
807		
808	A.8 Code Usage and API Documentation	31
809		
808	A.9 Installation and usage for development	34
809		
809	A.10 Theoretical motivation for post training in time series forecasting	35
809	A.11 Proof of the <i>Upper Bound on the Risk of the Corrected Prediction Theorem</i>	36

ABSTRACT

This supplementary material provides an extended discussion and additional details supporting the main paper on *Human-in-the-Loop Adaptive Optimization for Improved Time Series Forecasting*. We first delve deeper into the mathematical formulation of the different actions used in our framework, offering visualizations to better illustrate their roles and impacts on model performance.

Next, we provide an in-depth exploration of the adaptive optimization algorithms employed within our approach, detailing their integration into state-of-the-art time series forecasting models. Supplementary experiments are included to showcase the effectiveness of our adaptive optimization-enhanced models across various datasets, comparing them against baseline methods to highlight performance improvements.

Human feedback is also a central aspect of our framework. In this section, we demonstrate how human feedback can be integrated into the post-training process through several real-world examples, illustrating the subjective nature of human input and its positive impact on model fine-tuning.

Finally, we offer detailed instructions on how to reproduce the experiments and results presented in this work. This includes guidance on using the provided code and graphical interface, enabling users to easily test and customize our framework for their own time series forecasting tasks. All code and resources are made publicly available for further exploration and use by the research community.

A.1 MATHEMATICAL DEFINITIONS AND VISUALIZATIONS OF THE POOL OF ACTIONS

Before presenting the mathematical definitions in the table, let's define the notation used in the transformations:

- \mathbf{x} : The original time series or predictions (before transformation), where each x_t is the value at time t .
- \mathbf{y} : The transformed time series or predictions, resulting from applying one of the post-training actions.
- x_t : The value at time step t in the original time series.
- y_t : The transformed value at time step t in the new series.
- x_{\max} : The maximum value in the time series \mathbf{x} across all time steps.
- x_{\min} : The minimum value in the time series \mathbf{x} across all time steps.
- \bar{x} : The average value of the time series \mathbf{x} over all time steps.
- Q_{δ} : The δ -th quantile of the values in \mathbf{x} , which corresponds to the value at the specified percentile of the distribution of \mathbf{x} .
- Δ : The amount by which to shift the time series in the "Shift Series" action (in terms of time steps).
- s : The slope parameter for adding a linear trend to the time series, representing a change in the amplitude of the series over time.
- b : The intercept parameter for adding a linear trend to the time series, adjusting the average level of the series.
- f : The factor used in scaling operations, such as scaling the amplitude or adjusting the minimum/maximum values.
- σ : The standard deviation parameter for noise addition, influencing the spread of the generated noise.
- t : The time step index, which ranges from 1 to H , where H is the total number of time steps (the horizon) in the time series.

The following table summarizes each action's mathematical operation and the continuous parameters involved, along with their respective ranges.

These post-training actions modify time series predictions through mathematical transformations targeting trends, amplitudes, and frequency/phase. Each transformation is defined mathematically, with adjustable parameters like scaling factors and thresholds to optimize performance.

Action Name	Mathematical Definition	Continuous Parameters (Range)
Trend Modifications		
Linear Trend Slope	$\mathbf{y} = \mathbf{x} + \left(\frac{s}{100} \cdot (x_{\max} - x_{\min}) \right) \cdot t$	$s \in (-5, 5), t \in [H]$
Linear Trend Intercept	$\mathbf{y} = \mathbf{x} + \left(\frac{b}{100} \cdot \bar{x} \right)$	$b \in (-5, 5)$
Piecewise Scaling		
Piecewise Scale High	$\mathbf{y} = \mathbf{x} \cdot \left(1 + \frac{f}{100} \right)$ for $x_t \leq Q_\delta$	$\delta \in (70, 100), f \in (-1, 10)$
Piecewise Scale Low	$\mathbf{y} = \mathbf{x} \cdot \left(1 + \frac{f}{100} \right)$ for $x_t > Q_\delta$	$\delta \in (0, 30), f \in (-1, 10)$
Frequency and Phase		
Swap Series	$y_t = -(\mathbf{x} - \bar{x}) + \bar{x}$	None
Shift Series	$y_t = x_{t+\Delta}$	$\Delta \in (-200, 200)$
Amplitude Modifications		
Scale Amplitude	$\mathbf{y} = \mathbf{x} \cdot \left(1 + \frac{f}{100} \right)$	$f \in (-5, 5)$
Add Noise	$\mathbf{y} = \mathbf{x} + \epsilon$ where $\epsilon \sim \mathcal{N}(0, \frac{\sigma}{100} \cdot x_t)$	$\sigma \in (10, 30)$
Increase Minimum Factor	$\mathbf{y} = \mathbf{x} \cdot (1 + \frac{f}{100})$ for $x_t \leq Q_{10\%}$	$f \in (-1, 10)$

Table 4: Mathematical definitions and continuous parameters for each post-training action. The range for each parameter is specified to guide the tuning of each transformation. Note: x_t is the initial prediction and y_t is the transformed prediction for each sample and each dimension. x_{\max} and x_{\min} are minimum and maximum values of x_t over all horizons H and \bar{x} is the average value. Q_δ is the δ -quantile of the vector \mathbf{x} .

Figure 7 shows the original time series alongside the transformed series, with each subplot illustrating a different post-training action applied.

A.2 DETAILS ON EXPERIMENTAL SETUP: DATASETS AND MODELS

A.2.1 DATASETS

In this section, we provide a summary of the datasets used in our analysis. The following table outlines the dataset names, their sources, key characteristics, and the corresponding references for the papers that describe each dataset.

Table 5: Datasets Overview

Dataset Name	Source and Reference	Characteristics
ETTh1	ETTh (Electricity) Benchmark Zhou et al. (2021)	1-hour-level time-series with 6 features and "oil temperature" as the target. Train/val/test split: 12/4/4 months.
ETTh2	ETTh (Electricity) Benchmark Zhou et al. (2021)	1-hour-level time-series with 6 features and "oil temperature" as the target. Includes more features than ETTh1.
ETTm1	ETTh (Electricity) Benchmark Zhou et al. (2021)	15-minute-level time-series with 6 features and "oil temperature" as the target. Train/val/test split: 12/4/4 months.

Datasets Overview (Continued)		
Dataset Name	Source and Reference	Characteristics
ETTm2	ETTh (Electricity) Benchmark Zhou et al. (2021)	15-minute-level time-series, similar to ETTm1, with different subsets for long-term forecasting.
Dominick	Open TS Benchmark Qiu et al. (2024)	115704 weekly time series representing the profit of individual stock keeping units from a retailer.
Nature	Open TS Benchmark Qiu et al. (2024)	
Human	Open TS Benchmark Qiu et al. (2024)	Time-series data for human activity recognition, captured by wearable devices.
NASDAQ	Open TS Benchmark Qiu et al. (2024)	Stock market data from NASDAQ. Used for financial forecasting challenges.
KDD Cup	Open TS Benchmark Qiu et al. (2024)	
Pedestrian	Open TS Benchmark Qiu et al. (2024)	Pedestrian count data from urban settings, used for mobility prediction.
Tourism	Open TS Benchmark Qiu et al. (2024)	Tourism demand data, used for forecasting seasonal trends.
Vehicle Trips	Open TS Benchmark Qiu et al. (2024)	Vehicle trip data, used for urban mobility and traffic pattern forecasting.

A.2.2 TIME SERIES MODELS

In this work, we utilize several state-of-the-art time series forecasting models, all of which are part of the framework described in [Liu et al. \(2024b\)](#). These models are trained for 10 epochs, with early stopping applied on the validation set to prevent overfitting. Below, we briefly describe each of the models used:

- **Autoformer** [Wu et al. \(2021\)](#): A deep learning model designed to capture long-term dependencies and seasonality in time-series data by leveraging an attention mechanism.
- **Crossformer** [Zhang & Yan \(2023\)](#): This model integrates cross-attention mechanisms to effectively model both long-range and local dependencies in time-series forecasting.
- **PatchTST** [Nie et al. \(2023\)](#): A vision transformer-based model that divides time-series data into patches to capture temporal dependencies, providing superior performance in forecasting.
- **DLinear** [Zeng et al. \(2023\)](#): A linear decomposition model that separates the time series into trend and seasonal components for more interpretable and efficient forecasting.
- **Informer** [Zhou et al. \(2021\)](#): A transformer-based model that focuses on efficiency for long-term forecasting by using a self-attention mechanism and probabilistic forecast outputs.
- **SegRNN** [Lin et al. \(2023\)](#): A sequential deep learning model that combines segmentation with recurrent neural networks to handle irregular time-series data.

Each of these models has demonstrated strong performance in time series forecasting tasks, and we have used them to compare their abilities on the datasets described earlier.

A.3 MORE EXPERIMENTS ON THE REINFORCEMENT AUTOMATED LOOP

A.3.1 ROBUSTNESS ANALYSIS WITH RESPECT TO VALIDATION SETS

In our framework, the choice of the validation set is quite important. For well-known benchmark datasets like ETTh1, ETTh2, ETTm1, and ETTm2, we use the provided validation sets as specified

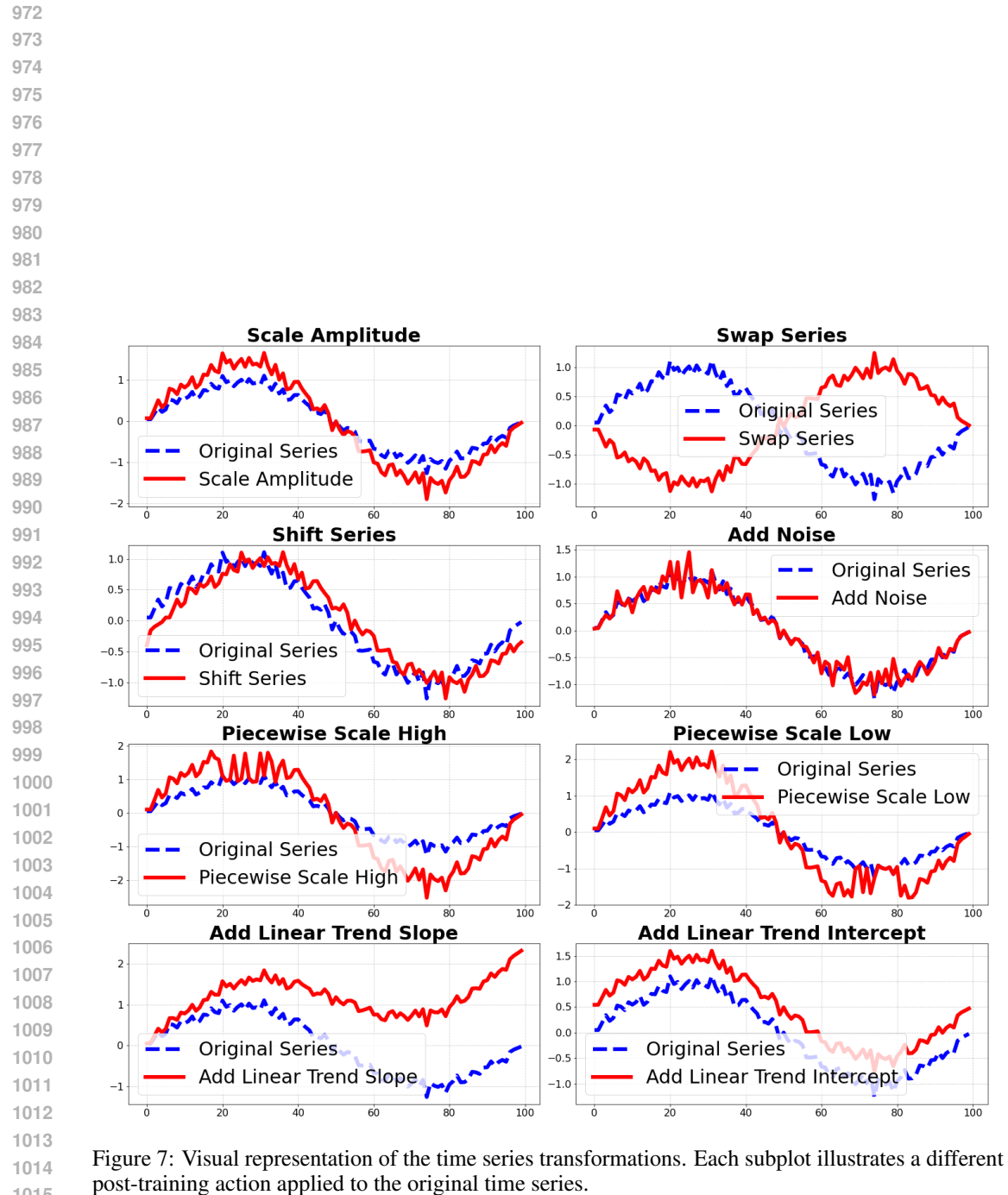
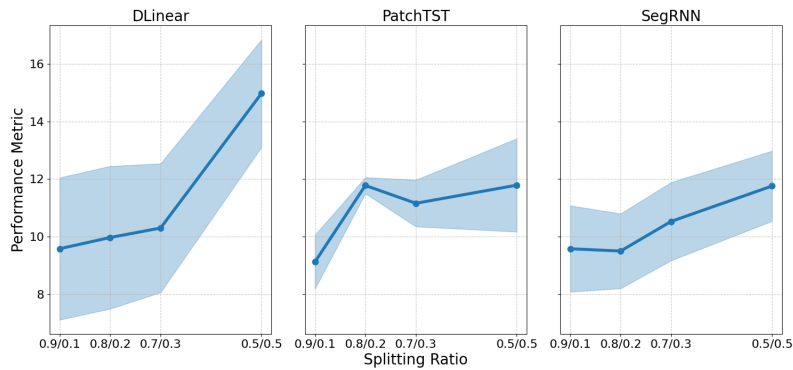


Figure 7: Visual representation of the time series transformations. Each subplot illustrates a different post-training action applied to the original time series.

1026 in the dataset documentation. For datasets without a predefined validation set, we split the training
1027 data temporally, using 30% of the data for validation, in line with common practices.
1028

1029 To assess the robustness of our approach, we conduct additional experiments on the ETTm1 dataset.
1030 While ETTm1 provides an explicit validation set, we discard it for this analysis and perform our own
1031 temporal split. This allows us to investigate how model performance varies with different validation
1032 set sizes. We experiment with three models *DLinear*, *PatchTST*, and *SegRNN* and test multiple
1033 validation set sizes, from smaller to larger subsets. The results reveal a consistent improvement of
1034 approximately 10% as the validation set size increases, with a monotonic improvement over larger
1035 validation sets observed across all models.
1036

1037 Each experiment is repeated 5 times, with train-validation splits shuffled to ensure robustness. The
1038 standard deviation is shown as a shaded region around the mean performance, providing a clear view
1039 of variability.
1040



1051 Figure 8: Quantitative MSE reduction (Performance metric) with respect to validation set size for
1052 *DLinear*, *PatchTST*, and *SegRNN*. We observe an MSE reduction of around 10% across different
1053 validation splits.
1054

1055 A.3.2 QUANTITATIVE ANALYSIS OF THE OPTIMIZATION PROCESS

1056 We present a qualitative analysis of the optimization process, illustrating the improvement in forecasting
1057 at different stages. The initial forecast is shown in red, representing the model’s performance at
1058 the beginning of the optimization. The middle prediction, made after 5 episodes, is also shown to
1059 demonstrate the progress. Finally, the forecast after the optimization process is completed shows the
1060 model’s final performance.
1061

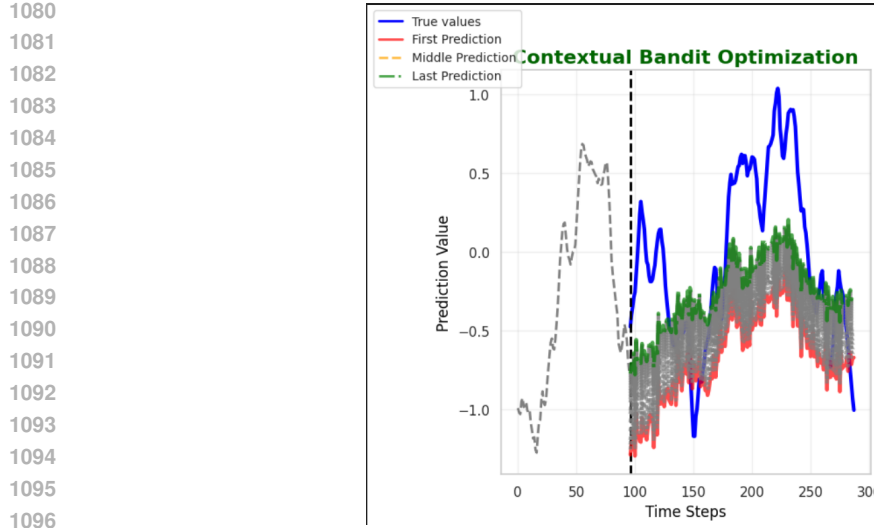
1062 The model used for this prediction is *PatchTST*, and the dataset is ETTm1. In black, we highlight all
1063 the unsuccessful actions attempted during the optimization process.
1064

1065 From this analysis, we can clearly observe the improvement in forecast accuracy over time, driven by
1066 the optimization process, which refines the predictions based on a fixed set of actions.
1067

1068 A.3.3 COMPARISON BETWEEN OPTIMIZATION STRATEGY OVER THE POOL OF ACTIONS

1069 We compare the performance of four different classes of algorithms:
1070

- 1071 1. **Random search** where each discrete action is evaluated by randomly sampling continuous
1072 parameters and selecting the best-performing configuration.
- 1073 2. **Bandit algorithm**, which considers each class of actions as an arm and optimizes using line
1074 search the parameter called SH-HPO.
- 1075 3. **Reinforcement learning algorithm (PPO)**, which discretizes the set of actions and imple-
1076 ments the PPO algorithm (Schulman et al., 2017) denoted RL (PPO).
- 1077 4. **Genetic algorithm (GA)** (Sampson, 1976), which discretizes the set of actions and performs
1078 a genetic algorithm denoted GA.



1080
1081
1082
1083
1084
1085
1086
1087
1088
1089
1090
1091
1092
1093
1094
1095
1096
1097
1098
1099
1100
1101
1102
1103
1104
1105
1106
1107
1108
1109
1110
1111
1112
1113
1114
1115
1116
1117
1118
1119
1120
1121
1122
1123
1124
1125
1126
1127
1128
1129
1130
1131
1132
1133

Figure 9: Qualitative improvement during the optimization process. The base learner is PatchTST on *ETTm1*. The validation set is the one explicitly provided by the benchmark. One sample from a specific channel is provided for illustration.

We present the result for several time series models and for five different datasets in Table 6.

The metric used to measure the efficiency of post-training is the relative decrease in Mean Squared Error (MSE) observed after post-training. Specifically, given the MSE before post-training, MSE_{before} , and the MSE after post-training, MSE_{after} , the relative decrease in MSE, \mathcal{M} , is calculated as:

$$\mathcal{M} = \frac{MSE_{\text{before}} - MSE_{\text{after}}}{MSE_{\text{before}}} \quad (2)$$

A positive value of \mathcal{M} indicates that post-training has reduced the MSE, with larger positive values signifying greater improvement. Conversely, a negative value indicates degradation compared to the initial prediction.

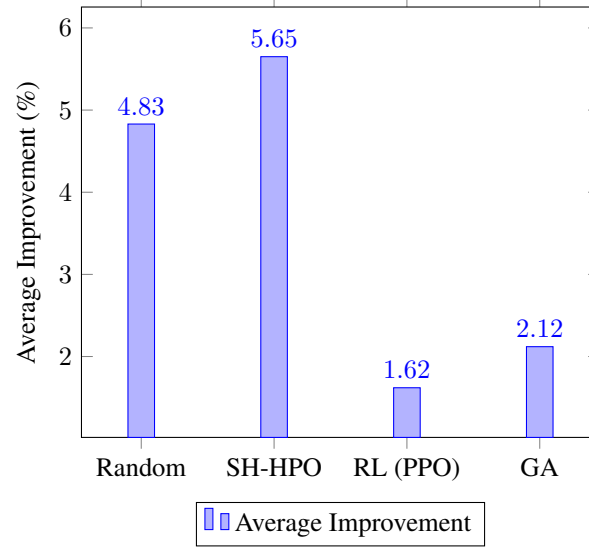


Figure 10: Average improvement across all models and datasets for each method.

1134
 1135
 1136
 1137
 1138
 1139
 1140
 1141
 1142
 1143
 1144
 1145
 1146
 1147
 1148
 1149
 1150
 1151
 1152
 1153
 1154
 1155
 1156
 1157
 1158
 1159
 1160
 1161
 1162
 1163
 1164
 1165
 1166
 1167
 1168
 1169
 1170
 1171
 1172
 1173
 1174
 1175
 1176
 1177
 1178
 1179
 1180
 1181
 1182
 1183
 1184
 1185
 1186
 1187

Models	Datasets	Random	SH-HPO	RL (PPO)	GA
Autoformer	ETTh1 (96)	12.77%	19.85%	2.71%	6.76%
	ETTh1 (192)	18.42%	17.32%	3.14%	6.20%
	ETTh1 (336)	13.09%	12.91%	3.54%	4.43%
	ETTh1 (792)	24.48%	27.26%	4.02%	6.96%
	Average	17.19%	19.34%	3.35%	6.09%
Crossformer	ETTh1 (96)	5.49%	4.01%	2.71%	0.16%
	ETTh1 (192)	2.05%	3.80%	1.71%	3.48%
	ETTh1 (336)	3.13%	3.13%	0.14%	1.37%
	ETTh1 (792)	2.53%	0.17%	-0.14%	1.07%
	Average	3.30%	2.78%	1.11%	1.52%
PatchTST	ETTh1 (96)	-0.99%	0.15%	0.40%	0.62%
	ETTh1 (192)	-0.06%	-1.13%	0.12%	0.23%
	ETTh1 (336)	-3.13%	0.23%	0.41%	0.19%
	ETTh1 (772)	-1.12%	-2.50%	0.12%	0.14%
	Average	-1.33%	-0.81%	0.26%	0.29%
SegRNN	ETTh1 (96)	0.80%	1.22%	0.13%	0.06%
	ETTh1 (192)	1.24%	1.56%	0.73%	0.68%
	ETTh1 (336)	2.38%	3.76%	0.71%	0.36%
	ETTh1 (772)	2.39%	3.81%	0.87%	1.26%
	Average	1.70%	2.59%	0.61%	0.59%
DLinear	ETTh1 (96)	1.50%	1.40%	0.97%	1.24%
	ETTh1 (192)	2.03%	2.18%	1.39%	2.35%
	ETTh1 (336)	2.96%	5.07%	4.62%	3.96%
	ETTh1 (772)	1.33%	-2.37%	1.82%	-1.11%
	Average	1.96%	1.57%	2.20%	1.61%
Informer	ETTh1 (96)	12.98%	6.83%	6.12%	4.87%
	ETTh1 (192)	8.89%	7.28%	3.74%	2.17%
	ETTh1 (336)	1.68%	4.01%	3.81%	2.49%
	ETTh1 (772)	-3.80%	3.61%	0.26%	0.94%
	Average	4.94%	5.43%	3.48%	2.62%
iTransformer	ETTh1 (96)	2.16%	4.83%	0.41%	1.05%
	ETTh1 (192)	2.79%	1.89%	1.26%	1.03%
	ETTh1 (336)	3.22%	4.01%	1.32%	1.78%
	ETTh1 (772)	4.23%	4.67%	2.34%	2.15%
	Average	3.10%	3.85%	1.33%	1.50%
Overall Average		4.83%	5.65%	1.62%	2.12%

Table 6: Results of applying different algorithms (Random, SH-HPO, RL (PPO), GA) to various time series forecasting models and datasets. Each cell shows the observed improvement for the respective algorithm, model, and dataset. The improvements are measured in percentage points.

A.3.4 EXPERIMENTS FOR THE SH-HPO ON ALL DATASETS AND HORIZONS

In the table, for each dataset, we evaluate performance at different horizon lengths (96, 192, 336, and 720), which are shown in the first four rows. The last row for each dataset represents the average performance improvement across all horizon lengths.

Methods	Autoformer	Crossformer	iTransformer	PatchTST	DLinear	SegRNN	Informer
<i>ETTh1</i>	$0.52 \pm 0.04 \rightarrow 0.45 \pm 0.03$ (12.94%)	$0.41 \pm 0.02 \rightarrow 0.39 \pm 0.01$ (3.41%)	$0.41 \pm 0.02 \rightarrow 0.40 \pm 0.01$ (1.97%)	$0.40 \pm 0.02 \rightarrow 0.41 \pm 0.01$ (-1.31%)	$0.41 \pm 0.02 \rightarrow 0.40 \pm 0.01$ (1.47%)	$0.39 \pm 0.02 \rightarrow 0.38 \pm 0.01$ (1.22%)	$0.57 \pm 0.02 \rightarrow 0.56 \pm 0.01$ (1.55%)
	$0.59 \pm 0.03 \rightarrow 0.48 \pm 0.02$ (17.75%)	$0.48 \pm 0.02 \rightarrow 0.46 \pm 0.02$ (3.43%)	$0.45 \pm 0.03 \rightarrow 0.44 \pm 0.02$ (2.77%)	$0.44 \pm 0.03 \rightarrow 0.44 \pm 0.02$ (-0.94%)	$0.46 \pm 0.03 \rightarrow 0.45 \pm 0.02$ (2.15%)	$0.43 \pm 0.03 \rightarrow 0.42 \pm 0.02$ (1.58%)	$0.67 \pm 0.03 \rightarrow 0.62 \pm 0.02$ (7.10%)
	$0.65 \pm 0.02 \rightarrow 0.57 \pm 0.01$ (11.51%)	$0.59 \pm 0.02 \rightarrow 0.58 \pm 0.01$ (0.67%)	$0.49 \pm 0.02 \rightarrow 0.47 \pm 0.01$ (3.54%)	$0.47 \pm 0.02 \rightarrow 0.48 \pm 0.01$ (-3.38%)	$0.50 \pm 0.02 \rightarrow 0.48 \pm 0.01$ (2.58%)	$0.50 \pm 0.02 \rightarrow 0.47 \pm 0.01$ (1.31%)	$0.70 \pm 0.02 \rightarrow 0.68 \pm 0.01$ (2.56%)
	$0.71 \pm 0.02 \rightarrow 0.53 \pm 0.03$ (24.85%)	$0.70 \pm 0.02 \rightarrow 0.68 \pm 0.01$ (2.76%)	$0.48 \pm 0.02 \rightarrow 0.47 \pm 0.01$ (2.05%)	$0.55 \pm 0.02 \rightarrow 0.56 \pm 0.01$ (-3.37%)	$0.51 \pm 0.02 \rightarrow 0.50 \pm 0.01$ (-0.68%)	$0.55 \pm 0.02 \rightarrow 0.52 \pm 0.01$ (1.04%)	$0.75 \pm 0.02 \rightarrow 0.74 \pm 0.01$ (0.75%)
	$0.61 \pm 0.01 \rightarrow 0.51 \pm 0.02$ (16.76%)	$0.54 \pm 0.01 \rightarrow 0.52 \pm 0.01$ (2.20%)	$0.45 \pm 0.01 \rightarrow 0.44 \pm 0.01$ (2.58%)	$0.46 \pm 0.01 \rightarrow 0.47 \pm 0.01$ (-2.25%)	$0.47 \pm 0.01 \rightarrow 0.45 \pm 0.01$ (1.38%)	$0.47 \pm 0.01 \rightarrow 0.45 \pm 0.01$ (1.31%)	$0.67 \pm 0.01 \rightarrow 0.65 \pm 0.01$ (3.00%)
<i>ETTh2</i>	$0.55 \pm 0.02 \rightarrow 0.44 \pm 0.01$ (20.87%)	$1.10 \pm 0.02 \rightarrow 1.04 \pm 0.01$ (5.38%)	$0.33 \pm 0.02 \rightarrow 0.32 \pm 0.01$ (2.45%)	$0.32 \pm 0.02 \rightarrow 0.31 \pm 0.01$ (3.23%)	$0.38 \pm 0.02 \rightarrow 0.33 \pm 0.01$ (15.12%)	$0.31 \pm 0.02 \rightarrow 0.30 \pm 0.01$ (3.51%)	$0.38 \pm 0.02 \rightarrow 0.37 \pm 0.01$ (1.89%)
	$0.78 \pm 0.03 \rightarrow 0.64 \pm 0.02$ (18.65%)	$1.59 \pm 0.03 \rightarrow 1.58 \pm 0.02$ (0.58%)	$0.40 \pm 0.03 \rightarrow 0.39 \pm 0.02$ (1.60%)	$0.40 \pm 0.03 \rightarrow 0.39 \pm 0.02$ (1.87%)	$0.50 \pm 0.03 \rightarrow 0.47 \pm 0.02$ (6.54%)	$0.39 \pm 0.03 \rightarrow 0.38 \pm 0.02$ (-5.88%)	$0.51 \pm 0.03 \rightarrow 0.47 \pm 0.02$ (7.13%)
	$0.75 \pm 0.02 \rightarrow 0.63 \pm 0.01$ (16.69%)	$6.57 \pm 0.02 \rightarrow 6.57 \pm 0.01$ (0.00%)	$0.44 \pm 0.02 \rightarrow 0.43 \pm 0.01$ (2.98%)	$0.43 \pm 0.02 \rightarrow 0.44 \pm 0.01$ (-2.40%)	$0.61 \pm 0.02 \rightarrow 0.57 \pm 0.01$ (6.15%)	$0.50 \pm 0.02 \rightarrow 0.47 \pm 0.01$ (3.61%)	$0.46 \pm 0.02 \rightarrow 0.44 \pm 0.01$ (3.84%)
	$0.55 \pm 0.02 \rightarrow 0.52 \pm 0.01$ (5.69%)	$0.55 \pm 0.02 \rightarrow 0.52 \pm 0.01$ (-0.01%)	$0.49 \pm 0.02 \rightarrow 0.48 \pm 0.01$ (4.13%)	$0.43 \pm 0.02 \rightarrow 0.40 \pm 0.01$ (5.05%)	$0.85 \pm 0.02 \rightarrow 0.79 \pm 0.01$ (6.70%)	$0.55 \pm 0.02 \rightarrow 0.52 \pm 0.01$ (1.31%)	$0.43 \pm 0.02 \rightarrow 0.42 \pm 0.01$ (0.44%)
	$0.65 \pm 0.01 \rightarrow 0.55 \pm 0.01$ (15.48%)	$0.60 \pm 0.01 \rightarrow 0.57 \pm 0.01$ (3.7%)	$0.60 \pm 0.01 \rightarrow 0.57 \pm 0.01$ (4.0%)	$0.60 \pm 0.01 \rightarrow 0.57 \pm 0.01$ (4.2%)	$0.60 \pm 0.01 \rightarrow 0.57 \pm 0.01$ (3.8%)	$0.60 \pm 0.01 \rightarrow 0.57 \pm 0.01$ (3.8%)	$0.60 \pm 0.01 \rightarrow 0.57 \pm 0.01$ (3.9%)
<i>ETTm1</i>	$0.43 \pm 0.02 \rightarrow 0.40 \pm 0.01$ (3.73%)	$0.39 \pm 0.02 \rightarrow 0.38 \pm 0.01$ (2.60%)	$0.21 \pm 0.02 \rightarrow 0.20 \pm 0.01$ (2.52%)	$0.36 \pm 0.02 \rightarrow 0.34 \pm 0.01$ (4.53%)	$0.37 \pm 0.02 \rightarrow 0.35 \pm 0.01$ (5.05%)	$0.35 \pm 0.02 \rightarrow 0.34 \pm 0.01$ (2.71%)	$0.71 \pm 0.02 \rightarrow 0.64 \pm 0.01$ (9.98%)
	$0.67 \pm 0.03 \rightarrow 0.62 \pm 0.02$ (6.31%)	$0.53 \pm 0.03 \rightarrow 0.50 \pm 0.02$ (5.24%)	$0.27 \pm 0.03 \rightarrow 0.25 \pm 0.02$ (2.42%)	$0.38 \pm 0.03 \rightarrow 0.37 \pm 0.02$ (2.27%)	$0.40 \pm 0.03 \rightarrow 0.38 \pm 0.02$ (3.62%)	$0.38 \pm 0.03 \rightarrow 0.37 \pm 0.02$ (2.34%)	$0.72 \pm 0.03 \rightarrow 0.70 \pm 0.02$ (2.92%)
	$0.73 \pm 0.02 \rightarrow 0.68 \pm 0.01$ (7.29%)	$0.72 \pm 0.02 \rightarrow 0.68 \pm 0.01$ (5.14%)	$0.33 \pm 0.02 \rightarrow 0.31 \pm 0.01$ (5.96%)	$0.41 \pm 0.02 \rightarrow 0.40 \pm 0.01$ (0.84%)	$0.42 \pm 0.02 \rightarrow 0.40 \pm 0.01$ (3.66%)	$0.50 \pm 0.02 \rightarrow 0.47 \pm 0.01$ (3.7%)	$0.73 \pm 0.02 \rightarrow 0.71 \pm 0.01$ (2.37%)
	$0.78 \pm 0.02 \rightarrow 0.70 \pm 0.01$ (9.83%)	$0.96 \pm 0.02 \rightarrow 0.85 \pm 0.01$ (0.89%)	$0.42 \pm 0.02 \rightarrow 0.39 \pm 0.01$ (0.88%)	$0.46 \pm 0.02 \rightarrow 0.45 \pm 0.01$ (2.8%)	$0.48 \pm 0.02 \rightarrow 0.46 \pm 0.01$ (3.97%)	$0.55 \pm 0.02 \rightarrow 0.52 \pm 0.01$ (2.7%)	$0.84 \pm 0.02 \rightarrow 0.77 \pm 0.01$ (7.56%)
	$0.60 \pm 0.01 \rightarrow 0.57 \pm 0.01$ (7.37%)	$0.60 \pm 0.01 \rightarrow 0.57 \pm 0.01$ (3.7%)	$0.60 \pm 0.01 \rightarrow 0.57 \pm 0.01$ (4.0%)	$0.60 \pm 0.01 \rightarrow 0.57 \pm 0.01$ (4.2%)	$0.60 \pm 0.01 \rightarrow 0.57 \pm 0.01$ (3.8%)	$0.60 \pm 0.01 \rightarrow 0.57 \pm 0.01$ (3.8%)	$0.60 \pm 0.01 \rightarrow 0.57 \pm 0.01$ (3.9%)
<i>ETTm2</i>	$0.27 \pm 0.02 \rightarrow 0.24 \pm 0.01$ (7.87%)	$0.33 \pm 0.02 \rightarrow 0.31 \pm 0.01$ (4.01%)	$0.46 \pm 0.02 \rightarrow 0.43 \pm 0.01$ (3.73%)	$0.20 \pm 0.02 \rightarrow 0.19 \pm 0.01$ (3.99%)	$0.21 \pm 0.02 \rightarrow 0.19 \pm 0.01$ (8.00%)	$0.19 \pm 0.02 \rightarrow 0.18 \pm 0.01$ (3.24%)	$0.25 \pm 0.02 \rightarrow 0.23 \pm 0.01$ (5.35%)
	$0.42 \pm 0.03 \rightarrow 0.32 \pm 0.02$ (22.58%)	$0.87 \pm 0.03 \rightarrow 0.45 \pm 0.02$ (4.8%)	$0.48 \pm 0.03 \rightarrow 0.45 \pm 0.02$ (6.18%)	$0.26 \pm 0.03 \rightarrow 0.24 \pm 0.02$ (7.69%)	$0.31 \pm 0.03 \rightarrow 0.25 \pm 0.02$ (18.97%)	$0.25 \pm 0.03 \rightarrow 0.24 \pm 0.02$ (5.20%)	$0.31 \pm 0.03 \rightarrow 0.28 \pm 0.02$ (7.88%)
	$0.46 \pm 0.02 \rightarrow 0.35 \pm 0.01$ (23.54%)	$0.99 \pm 0.02 \rightarrow 0.47 \pm 0.01$ (3.6%)	$0.50 \pm 0.02 \rightarrow 0.47 \pm 0.01$ (5.96%)	$0.32 \pm 0.02 \rightarrow 0.29 \pm 0.01$ (7.82%)	$0.38 \pm 0.02 \rightarrow 0.33 \pm 0.01$ (13.81%)	$0.50 \pm 0.02 \rightarrow 0.47 \pm 0.01$ (3.7%)	$0.37 \pm 0.02 \rightarrow 0.34 \pm 0.01$ (7.04%)
	$1.15 \pm 0.02 \rightarrow 0.84 \pm 0.01$ (27.00%)	$0.55 \pm 0.02 \rightarrow 0.52 \pm 0.01$ (3.1%)	$0.55 \pm 0.02 \rightarrow 0.52 \pm 0.01$ (7.51%)	$0.41 \pm 0.02 \rightarrow 0.38 \pm 0.01$ (7.36%)	$0.55 \pm 0.02 \rightarrow 0.52 \pm 0.01$ (6.78%)	$0.55 \pm 0.02 \rightarrow 0.52 \pm 0.01$ (2.7%)	$0.47 \pm 0.02 \rightarrow 0.43 \pm 0.01$ (6.99.9%)
	$0.60 \pm 0.01 \rightarrow 0.57 \pm 0.01$ (20.25%)	$3.82 \pm 0.01 \rightarrow 3.81 \pm 0.01$ (3.7%)	$0.60 \pm 0.01 \rightarrow 0.57 \pm 0.01$ (4.0%)	$0.60 \pm 0.01 \rightarrow 0.57 \pm 0.01$ (4.2%)	$0.60 \pm 0.01 \rightarrow 0.57 \pm 0.01$ (3.8%)	$0.60 \pm 0.01 \rightarrow 0.57 \pm 0.01$ (3.8%)	$0.60 \pm 0.01 \rightarrow 0.57 \pm 0.01$ (3.9%)
<i>Weather</i>	$0.46 \pm 0.02 \rightarrow 0.43 \pm 0.01$ (6.2%)	$0.46 \pm 0.02 \rightarrow 0.43 \pm 0.01$ (2.5%)	$0.19 \pm 0.02 \rightarrow 0.18 \pm 0.01$ (7.64%)	$0.21 \pm 0.02 \rightarrow 0.19 \pm 0.01$ (5.13%)	$0.46 \pm 0.02 \rightarrow 0.43 \pm 0.01$ (8.88%)	$0.46 \pm 0.02 \rightarrow 0.43 \pm 0.01$ (6.0%)	$0.46 \pm 0.02 \rightarrow 0.43 \pm 0.01$ (5.1%)
	$0.48 \pm 0.03 \rightarrow 0.45 \pm 0.02$ (5.4%)	$0.48 \pm 0.03 \rightarrow 0.45 \pm 0.02$ (4.8%)	$0.23 \pm 0.03 \rightarrow 0.21 \pm 0.02$ (7.89%)	$0.23 \pm 0.03 \rightarrow 0.21 \pm 0.02$ (6.09%)	$0.24 \pm 0.03 \rightarrow 0.22 \pm 0.02$ (8.14%)	$0.48 \pm 0.03 \rightarrow 0.45 \pm 0.02$ (5.0%)	$0.48 \pm 0.03 \rightarrow 0.45 \pm 0.02$ (5.3%)
	$0.50 \pm 0.02 \rightarrow 0.47 \pm 0.01$ (4.1%)	$0.50 \pm 0.02 \rightarrow 0.47 \pm 0.01$ (3.6%)	$0.50 \pm 0.02 \rightarrow 0.47 \pm 0.01$ (6.57%)	$0.29 \pm 0.02 \rightarrow 0.27 \pm 0.01$ (5.55%)	$0.29 \pm 0.02 \rightarrow 0.27 \pm 0.01$ (5.61%)	$0.50 \pm 0.02 \rightarrow 0.47 \pm 0.01$ (3.7%)	$0.50 \pm 0.02 \rightarrow 0.47 \pm 0.01$ (3.8%)
	$0.55 \pm 0.02 \rightarrow 0.52 \pm 0.01$ (2.4%)	$0.55 \pm 0.02 \rightarrow 0.52 \pm 0.01$ (3.1%)	$0.55 \pm 0.02 \rightarrow 0.52 \pm 0.01$ (8.92%)	$0.55 \pm 0.02 \rightarrow 0.52 \pm 0.01$ (7.44%)	$0.35 \pm 0.02 \rightarrow 0.33 \pm 0.01$ (4.07%)	$0.55 \pm 0.02 \rightarrow 0.52 \pm 0.01$ (2.7%)	$0.55 \pm 0.02 \rightarrow 0.52 \pm 0.01$ (2.9%)
	$0.60 \pm 0.01 \rightarrow 0.57 \pm 0.01$ (0.60%)	$0.60 \pm 0.01 \rightarrow 0.57 \pm 0.01$ (0.57%)	$0.60 \pm 0.01 \rightarrow 0.57 \pm 0.01$ (0.57%)	$0.60 \pm 0.01 \rightarrow 0.57 \pm 0.01$ (0.57%)	$0.60 \pm 0.01 \rightarrow 0.57 \pm 0.01$ (0.57%)	$0.60 \pm 0.01 \rightarrow 0.57 \pm 0.01$ (0.57%)	$0.60 \pm 0.01 \rightarrow 0.57 \pm 0.01$ (0.57%)

1242	(4.4%)	(3.7%)	(4.0%)	(4.2%)	(3.8%)	(3.8%)	(3.9%)
1243							
1244	1.22 \pm 0.02 \rightarrow 1.10 \pm 0.01	1.25 \pm 0.02 \rightarrow 1.25 \pm 0.01	1.40 \pm 0.02 \rightarrow 1.40 \pm 0.01	1.37 \pm 0.02 \rightarrow 1.37 \pm 0.01	1.34 \pm 0.02 \rightarrow 1.24 \pm 0.01	1.80 \pm 0.02 \rightarrow 1.39 \pm 0.01	1.26 \pm 1.23 \rightarrow 0.43 \pm 0.01
1245	(12.93%)	(0.00%)	(0.00%)	(0.00%)	(6.73%)	(22.76%)	(2.35%)
Dominick							
1246	1.31 \pm 0.03 \rightarrow 1.18 \pm 0.02	0.97 \pm 0.03 \rightarrow 0.97 \pm 0.02	1.05 \pm 0.03 \rightarrow 1.05 \pm 0.02	1.08 \pm 0.03 \rightarrow 1.08 \pm 0.02	1.03 \pm 0.03 \rightarrow 0.94 \pm 0.02	1.66 \pm 0.03 \rightarrow 1.20 \pm 0.02	0.92 \pm 0.03 \rightarrow 0.88 \pm 0.02
1247	(29.38%)	(0.00%)	(0.00%)	(0.00%)	(8.10%)	(27.52%)	(3.81%)
1248	1.43 \pm 0.02 \rightarrow 1.01 \pm 0.01	1.09 \pm 0.02 \rightarrow 1.06 \pm 0.01	1.23 \pm 0.02 \rightarrow 1.23 \pm 0.01	1.23 \pm 0.02 \rightarrow 1.13 \pm 0.01	1.25 \pm 0.02 \rightarrow 1.13 \pm 0.01	1.97 \pm 0.02 \rightarrow 1.39 \pm 0.01	1.15 \pm 0.02 \rightarrow 1.09 \pm 0.01
1249	(9.76%)	(2.56%)	(0.00%)	(8.01%)	(9.08%)	(28.94%)	(3.81%)
1250	1.55 \pm 0.02 \rightarrow 1.34 \pm 0.01	1.17 \pm 0.02 \rightarrow 1.15 \pm 0.01	1.30 \pm 0.02 \rightarrow 1.25 \pm 0.01	1.32 \pm 0.02 \rightarrow 1.22 \pm 0.01	1.32 \pm 0.02 \rightarrow 1.21 \pm 0.01	2.28 \pm 0.02 \rightarrow 1.60 \pm 0.01	1.26 \pm 0.02 \rightarrow 1.18 \pm 0.01
1251	(9.61%)	(1.41%)	(3.56%)	(7.34%)	(7.97%)	(29.63%)	(5.68%)
1252	1.38 \pm 0.01 \rightarrow 1.16 \pm 0.01	1.12 \pm 0.01 \rightarrow 1.10 \pm 0.01	1.25 \pm 0.01 \rightarrow 1.23 \pm 0.01	1.25 \pm 0.01 \rightarrow 1.20 \pm 0.01	1.24 \pm 0.01 \rightarrow 1.13 \pm 0.01	1.92 \pm 0.01 \rightarrow 1.40 \pm 0.01	1.14 \pm 0.01 \rightarrow 1.09 \pm 0.01
1253	(15.42%)	(1.00%)	(0.89%)	(3.83%)	(7.97%)	(27.21%)	(4.28%)
1254	0.37 \pm 0.02 \rightarrow 0.31 \pm 0.01	0.26 \pm 0.02 \rightarrow 0.22 \pm 0.01	0.18 \pm 0.02 \rightarrow 0.12 \pm 0.01	0.17 \pm 0.02 \rightarrow 0.11 \pm 0.01	0.36 \pm 0.02 \rightarrow 0.28 \pm 0.01	0.30 \pm 0.02 \rightarrow 0.25 \pm 0.01	0.13 \pm 0.02 \rightarrow 0.14 \pm 0.01
1255	(14.19%)	(13.66%)	(32.74%)	(35.22%)	(20.22%)	(15.68%)	(-2.76%)
Human							
1256	0.32 \pm 0.03 \rightarrow 0.26 \pm 0.02	0.26 \pm 0.03 \rightarrow 0.22 \pm 0.02	0.17 \pm 0.03 \rightarrow 0.12 \pm 0.02	0.14 \pm 0.03 \rightarrow 0.11 \pm 0.02	0.52 \pm 0.03 \rightarrow 0.24 \pm 0.02	0.28 \pm 0.03 \rightarrow 0.20 \pm 0.02	0.19 \pm 0.03 \rightarrow 0.14 \pm 0.02
1257	(16.59%)	(11.86%)	(24.88%)	(17.79%)	(52.35%)	(26.57%)	(25.19%)
1258	0.30 \pm 0.02 \rightarrow 0.17 \pm 0.01	0.29 \pm 0.02 \rightarrow 0.24 \pm 0.01	0.48 \pm 0.02 \rightarrow 0.19 \pm 0.01	0.52 \pm 0.02 \rightarrow 0.16 \pm 0.01	1.01 \pm 0.02 \rightarrow 0.28 \pm 0.01	0.56 \pm 0.02 \rightarrow 0.26 \pm 0.01	0.26 \pm 0.02 \rightarrow 0.19 \pm 0.01
1259	(40.52%)	(16.28%)	(58.95%)	(68.20%)	(71.56%)	(52.10%)	(25.10%)
1260	0.62 \pm 0.02 \rightarrow 0.56 \pm 0.01	0.40 \pm 0.02 \rightarrow 0.35 \pm 0.01	1.60 \pm 0.02 \rightarrow 0.18 \pm 0.01	1.66 \pm 0.02 \rightarrow 0.23 \pm 0.01	1.97 \pm 0.02 \rightarrow 0.25 \pm 0.01	1.27 \pm 0.02 \rightarrow 0.28 \pm 0.01	0.64 \pm 0.02 \rightarrow 0.38 \pm 0.01
1261	(9.67%)	(11.58%)	(88.50%)	(85.76%)	(87.30%)	(77.75%)	(40.17%)
1262	(20.24%)	(13.34%)	(51.26%)	(51.74%)	(57.85%)	(43.02%)	(21.93%)
1263	1.06 \pm 0.02 \rightarrow 0.83 \pm 0.01	0.71 \pm 0.02 \rightarrow 0.70 \pm 0.01	0.90 \pm 0.02 \rightarrow 0.74 \pm 0.01	0.94 \pm 0.02 \rightarrow 0.76 \pm 0.01	0.84 \pm 0.02 \rightarrow 0.77 \pm 0.01	0.92 \pm 0.02 \rightarrow 0.76 \pm 0.01	0.96 \pm 0.02 \rightarrow 0.77 \pm 0.01
1264	(20.98%)	(0.19%)	(17.14%)	(19.18%)	(7.81%)	(16.63%)	(19.59%)
KDD							
1265	1.20 \pm 0.03 \rightarrow 0.94 \pm 0.02	0.81 \pm 0.03 \rightarrow 0.81 \pm 0.02	1.08 \pm 0.03 \rightarrow 0.86 \pm 0.02	1.11 \pm 0.03 \rightarrow 0.88 \pm 0.02	0.93 \pm 0.03 \rightarrow 0.86 \pm 0.02	1.08 \pm 0.03 \rightarrow 0.87 \pm 0.02	1.08 \pm 0.03 \rightarrow 0.85 \pm 0.02
1266	(21.11%)	(-0.06%)	(19.98%)	(20.64%)	(7.24%)	(18.61%)	(20.86%)
1267	1.29 \pm 0.02 \rightarrow 0.98 \pm 0.01	0.84 \pm 0.02 \rightarrow 0.84 \pm 0.01	1.19 \pm 0.02 \rightarrow 0.93 \pm 0.01	1.21 \pm 0.02 \rightarrow 0.93 \pm 0.01	0.95 \pm 0.02 \rightarrow 0.87 \pm 0.01	1.17 \pm 0.02 \rightarrow 0.93 \pm 0.01	1.18 \pm 0.02 \rightarrow 0.96 \pm 0.01
1268	(23.58%)	(-0.16%)	(21.71%)	(22.58%)	(7.89%)	(19.71%)	(23.52%)
1269	1.47 \pm 0.02 \rightarrow 1.05 \pm 0.01	0.83 \pm 0.02 \rightarrow 0.83 \pm 0.01	1.33 \pm 0.02 \rightarrow 0.99 \pm 0.01	1.31 \pm 0.02 \rightarrow 0.88 \pm 0.01	1.01 \pm 0.02 \rightarrow 0.89 \pm 0.01	1.24 \pm 0.02 \rightarrow 0.97 \pm 0.01	1.28 \pm 0.02 \rightarrow 0.96 \pm 0.01
1270	(28.32%)	(0.00%)	(25.51%)	(24.92%)	(11.22%)	(21.63%)	(24.66%)
1271	1.29 \pm 0.01 \rightarrow 0.95 \pm 0.01	0.80 \pm 0.01 \rightarrow 0.80 \pm 0.01	1.13 \pm 0.01 \rightarrow 0.88 \pm 0.01	1.14 \pm 0.01 \rightarrow 0.89 \pm 0.01	0.93 \pm 0.01 \rightarrow 0.85 \pm 0.01	1.10 \pm 0.01 \rightarrow 0.88 \pm 0.01	1.12 \pm 0.01 \rightarrow 0.87 \pm 0.01
1272	(23.50%)	(-0.03%)	(21.09%)	(21.83%)	(8.54%)	(19.14%)	(22.15%)
1273	1.22 \pm 0.02 \rightarrow 0.79 \pm 0.01	0.28 \pm 0.02 \rightarrow 0.28 \pm 0.01	0.29 \pm 0.02 \rightarrow 0.28 \pm 0.01	0.27 \pm 0.02 \rightarrow 0.26 \pm 0.01	0.87 \pm 0.02 \rightarrow 0.80 \pm 0.01	1.04 \pm 0.02 \rightarrow 0.83 \pm 0.01	0.78 \pm 0.02 \rightarrow 0.70 \pm 0.01
1274	(35.00%)	(-1.74%)	(1.95%)	(1.37%)	(7.16%)	(19.90%)	(0.38%)
Nature							
1275	1.74 \pm 0.03 \rightarrow 1.19 \pm 0.02	0.63 \pm 0.03 \rightarrow 0.66 \pm 0.02	0.30 \pm 0.03 \rightarrow 0.29 \pm 0.02	0.24 \pm 0.03 \rightarrow 0.23 \pm 0.02	0.99 \pm 0.03 \rightarrow 0.95 \pm 0.02	1.05 \pm 0.03 \rightarrow 0.97 \pm 0.02	0.96 \pm 0.03 \rightarrow 0.95 \pm 0.02
1276	(31.15%)	(-3.91%)	(2.83%)	(2.38%)	(3.25%)	(6.86%)	(0.39%)
1277	1.01 \pm 0.02 \rightarrow 0.95 \pm 0.01	0.83 \pm 0.02 \rightarrow 0.81 \pm 0.01	0.30 \pm 0.02 \rightarrow 0.28 \pm 0.01	0.22 \pm 0.02 \rightarrow 0.20 \pm 0.01	0.98 \pm 0.02 \rightarrow 0.94 \pm 0.01	1.04 \pm 0.02 \rightarrow 0.98 \pm 0.01	0.95 \pm 0.02 \rightarrow 0.94 \pm 0.01
1278	(5.80%)	(1.10%)	(3.99%)	(4.75%)	(3.19%)	(5.33%)	(0.62%)
1279	(7.44%)	(-0.13%)	(4.30%)	(6.40%)	(3.65%)	(2.61%)	(2.06%)
1280	1.25 \pm 0.01 \rightarrow 0.96 \pm 0.01	0.65 \pm 0.01 \rightarrow 0.66 \pm 0.01	0.34 \pm 0.01 \rightarrow 0.33 \pm 0.01	0.26 \pm 0.01 \rightarrow 0.25 \pm 0.01	0.95 \pm 0.01 \rightarrow 0.91 \pm 0.01	1.02 \pm 0.01 \rightarrow 0.94 \pm 0.01	0.91 \pm 0.01 \rightarrow 0.90 \pm 0.01
1281	(21.69%)	(-1.17%)	(3.26%)	(3.72%)	(4.31%)	(8.67%)	(0.86%)
1282	0.72 \pm 0.02 \rightarrow 0.55 \pm 0.01	0.36 \pm 0.02 \rightarrow 0.36 \pm 0.01	0.51 \pm 0.02 \rightarrow 0.42 \pm 0.01	0.50 \pm 0.02 \rightarrow 0.42 \pm 0.01	0.56 \pm 0.02 \rightarrow 0.53 \pm 0.01	0.51 \pm 0.02 \rightarrow 0.43 \pm 0.01	0.57 \pm 0.02 \rightarrow 0.48 \pm 0.01
1283	(23.38%)	(-1.05%)	(16.14%)	(14.96%)	(5.24%)	(15.21%)	(15.20%)
NASDAQ							
1284	0.78 \pm 0.03 \rightarrow 0.62 \pm 0.02	0.41 \pm 0.03 \rightarrow 0.41 \pm 0.02	0.70 \pm 0.03 \rightarrow 0.56 \pm 0.02	0.67 \pm 0.03 \rightarrow 0.54 \pm 0.02	0.67 \pm 0.03 \rightarrow 0.62 \pm 0.02	0.67 \pm 0.03 \rightarrow 0.54 \pm 0.02	0.75 \pm 0.03 \rightarrow 0.61 \pm 0.02
1285	(19.76%)	(-0.24%)	(18.99%)	(18.08%)	(6.62%)	(18.34%)	(17.99%)
1286	(21.70%)	(-0.09%)	(19.70%)	(19.63%)	(8.13%)	(19.47%)	(21.48%)
1287	0.98 \pm 0.02 \rightarrow 0.76 \pm 0.01	0.51 \pm 0.02 \rightarrow 0.51 \pm 0.01	0.88 \pm 0.02 \rightarrow 0.70 \pm 0.01	0.87 \pm 0.02 \rightarrow 0.70 \pm 0.01	0.82 \pm 0.02 \rightarrow 0.75 \pm 0.01	0.87 \pm 0.02 \rightarrow 0.70 \pm 0.01	0.96 \pm 0.02 \rightarrow 0.91 \pm 0.01
1288	(24.72%)	(0.06%)	(24.26%)	(24.58%)	(10.40%)	(23.74%)	(23.76%)
1289	0.91 \pm 0.01 \rightarrow 0.70 \pm 0.01	0.46 \pm 0.01 \rightarrow 0.46 \pm 0.01	0.80 \pm 0.01 \rightarrow 0.63 \pm 0.01	0.79 \pm 0.01 \rightarrow 0.68 \pm 0.01	0.74 \pm 0.01 \rightarrow 0.68 \pm 0.01	0.78 \pm 0.01 \rightarrow 0.62 \pm 0.01	0.85 \pm 0.01 \rightarrow 0.79 \pm 0.01
1290	(22.39%)	(-0.33%)	(19.77%)	(14.76%)	(7.59%)	(19.19%)	(8.96%)
1291							
1292	0.38 \pm 0.02 \rightarrow 0.22 \pm 0.01	0.11 \pm 0.02 \rightarrow 0.11 \pm 0.01	0.09 \pm 0.02 \rightarrow 0.08 \pm 0.01	0.14 \pm 0.02 \rightarrow 0.13 \pm 0.01	0.33 \pm 0.02 \rightarrow 0.27 \pm 0.01	0.14 \pm 0.02 \rightarrow 0.13 \pm 0.01	0.21 \pm 0.02 \rightarrow 0.18 \pm 0.01
1293	(41.72%)	(-0.03%)	(2.85%)	(3.68%)	(18.21%)	(1.53%)	(18.38%)
Pedestrian							
1294	0.38 \pm 0.03 \rightarrow 0.24 \pm 0.02	0.13 \pm 0.03 \rightarrow 0.12 \pm 0.02	0.14 \pm 0.03 \rightarrow 0.12 \pm 0.02	0.22 \pm 0.03 \rightarrow 0.18 \pm 0.02	0.74 \pm 0.03 \rightarrow 0.63 \pm 0.02	0.20 \pm 0.03 \rightarrow 0.18 \pm 0.02	0.39 \pm 0.03 \rightarrow 0.33 \pm 0.02
1295	(34.76%)	(0.43%)	(11.79%)	(11.82%)	(14.79%)	(9.37%)	(15.51%)

1296	(41.30%)	(0.37%)	(12.15%)	(11.49%)	(13.38%)	(8.83%)	(18.22%)
1297	$0.55 \pm 0.02 \rightarrow 0.31 \pm 0.01$	$0.16 \pm 0.02 \rightarrow 0.15 \pm 0.01$	$0.18 \pm 0.02 \rightarrow 0.16 \pm 0.01$	$0.27 \pm 0.02 \rightarrow 0.25 \pm 0.01$	$0.77 \pm 0.02 \rightarrow 0.66 \pm 0.01$	$0.25 \pm 0.02 \rightarrow 0.22 \pm 0.01$	$0.38 \pm 0.02 \rightarrow 0.31 \pm 0.01$
1298	(42.27%)	(0.30%)	(10.94%)	(11.18%)	(13.88%)	(8.01%)	(19.35%)
1299	$0.46 \pm 0.01 \rightarrow 0.27 \pm 0.01$	$0.14 \pm 0.01 \rightarrow 0.13 \pm 0.01$	$0.14 \pm 0.01 \rightarrow 0.12 \pm 0.01$	$0.22 \pm 0.01 \rightarrow 0.19 \pm 0.01$	$0.69 \pm 0.01 \rightarrow 0.60 \pm 0.01$	$0.20 \pm 0.01 \rightarrow 0.18 \pm 0.01$	$0.33 \pm 0.01 \rightarrow 0.27 \pm 0.01$
1300	(40.01%)	(0.26%)	(9.43%)	(9.54%)	(14.20%)	(6.94%)	(15.87%)
1301	$0.38 \pm 0.02 \rightarrow 0.33 \pm 0.01$	$0.11 \pm 0.02 \rightarrow 0.08 \pm 0.01$	$0.16 \pm 0.02 \rightarrow 0.11 \pm 0.01$	$0.16 \pm 0.02 \rightarrow 0.11 \pm 0.01$	$0.34 \pm 0.02 \rightarrow 0.22 \pm 0.01$	$0.17 \pm 0.02 \rightarrow 0.08 \pm 0.01$	$0.17 \pm 0.02 \rightarrow 0.12 \pm 0.01$
1302	(12.79%)	(25.00%)	(26.16%)	(28.55%)	(33.74%)	(50.06%)	(27.43%)
1303	<i>Tourism</i>						
1304	$0.13 \pm 0.03 \rightarrow 0.10 \pm 0.02$	$0.08 \pm 0.03 \rightarrow 0.07 \pm 0.02$	$0.11 \pm 0.03 \rightarrow 0.10 \pm 0.02$	$0.12 \pm 0.03 \rightarrow 0.10 \pm 0.02$	$0.40 \pm 0.03 \rightarrow 0.17 \pm 0.02$	$0.20 \pm 0.03 \rightarrow 0.11 \pm 0.02$	$0.14 \pm 0.03 \rightarrow 0.10 \pm 0.02$
1305	(17.05%)	(8.79%)	(8.96%)	(3.10%)	(56.60%)	(43.12%)	(22.82%)
1306	$0.30 \pm 0.02 \rightarrow 0.31 \pm 0.01$	$0.15 \pm 0.02 \rightarrow 0.14 \pm 0.01$	$0.50 \pm 0.02 \rightarrow 0.26 \pm 0.01$	$0.50 \pm 0.02 \rightarrow 0.26 \pm 0.01$	$0.68 \pm 0.02 \rightarrow 0.37 \pm 0.01$	$0.33 \pm 0.02 \rightarrow 0.15 \pm 0.01$	$0.33 \pm 0.02 \rightarrow 0.31 \pm 0.01$
1307	(-3.60%)	(6.10%)	(47.99%)	(47.75%)	(44.29%)	(53.09%)	(4.90%)
1308	$0.18 \pm 0.02 \rightarrow 0.14 \pm 0.01$	$0.31 \pm 0.02 \rightarrow 0.29 \pm 0.01$	$0.48 \pm 0.02 \rightarrow 0.11 \pm 0.01$	$0.49 \pm 0.02 \rightarrow 0.11 \pm 0.01$	$0.66 \pm 0.02 \rightarrow 0.25 \pm 0.01$	$0.28 \pm 0.02 \rightarrow 0.15 \pm 0.01$	$0.26 \pm 0.02 \rightarrow 0.19 \pm 0.01$
1309	(17.30%)	(6.04%)	(77.23%)	(77.41%)	(61.01%)	(46.32%)	(27.16%)
1310	$0.24 \pm 0.01 \rightarrow 0.22 \pm 0.01$	$0.16 \pm 0.01 \rightarrow 0.14 \pm 0.01$	$0.31 \pm 0.01 \rightarrow 0.14 \pm 0.01$	$0.31 \pm 0.01 \rightarrow 0.14 \pm 0.01$	$0.52 \pm 0.01 \rightarrow 0.25 \pm 0.01$	$0.24 \pm 0.01 \rightarrow 0.12 \pm 0.01$	$0.22 \pm 0.01 \rightarrow 0.18 \pm 0.01$
1311	$1.40 \pm 0.02 \rightarrow 1.13 \pm 0.01$	$0.64 \pm 0.02 \rightarrow 0.62 \pm 0.01$	$0.89 \pm 0.02 \rightarrow 0.78 \pm 0.01$	$0.86 \pm 0.02 \rightarrow 0.71 \pm 0.01$	$1.24 \pm 0.02 \rightarrow 1.14 \pm 0.01$	$1.45 \pm 0.02 \rightarrow 0.72 \pm 0.01$	$1.15 \pm 0.02 \rightarrow 0.83 \pm 0.01$
1312	(19.00%)	(2.71%)	(11.63%)	(16.60%)	(7.46%)	(26.95%)	(8.02%)
1313	<i>Vehicle trips</i>						
1314	$1.39 \pm 0.03 \rightarrow 1.14 \pm 0.02$	$0.84 \pm 0.03 \rightarrow 0.85 \pm 0.02$	$0.81 \pm 0.03 \rightarrow 0.68 \pm 0.02$	$0.79 \pm 0.03 \rightarrow 0.69 \pm 0.02$	$1.25 \pm 0.03 \rightarrow 1.10 \pm 0.02$	$1.37 \pm 0.03 \rightarrow 0.77 \pm 0.02$	$1.05 \pm 0.03 \rightarrow 0.81 \pm 0.02$
1315	(17.78%)	(-2.23%)	(15.09%)	(11.95%)	(11.83%)	(21.34%)	(6.77%)
1316	$1.48 \pm 0.02 \rightarrow 1.18 \pm 0.01$	$0.95 \pm 0.02 \rightarrow 0.94 \pm 0.01$	$1.08 \pm 0.02 \rightarrow 0.87 \pm 0.01$	$1.02 \pm 0.02 \rightarrow 0.80 \pm 0.01$	$1.34 \pm 0.02 \rightarrow 1.11 \pm 0.01$	$1.78 \pm 0.02 \rightarrow 1.28 \pm 0.01$	$1.25 \pm 0.02 \rightarrow 1.04 \pm 0.01$
1317	(19.65%)	(0.82%)	(18.82%)	(20.85%)	(16.47%)	(27.59%)	(16.29%)
1318	$1.30 \pm 0.02 \rightarrow 1.09 \pm 0.01$	$0.90 \pm 0.02 \rightarrow 0.87 \pm 0.01$	$1.32 \pm 0.02 \rightarrow 1.01 \pm 0.01$	$1.27 \pm 0.02 \rightarrow 0.98 \pm 0.01$	$1.59 \pm 0.02 \rightarrow 1.24 \pm 0.01$	$2.13 \pm 0.02 \rightarrow 1.42 \pm 0.01$	$1.40 \pm 0.02 \rightarrow 1.12 \pm 0.01$
1319	(16.09%)	(2.27%)	(23.03%)	(22.63%)	(21.70%)	(33.07%)	(19.63%)
1320	$1.39 \pm 0.01 \rightarrow 1.13 \pm 0.01$	$0.83 \pm 0.01 \rightarrow 0.82 \pm 0.01$	$1.02 \pm 0.01 \rightarrow 0.84 \pm 0.01$	$0.98 \pm 0.01 \rightarrow 0.80 \pm 0.01$	$1.35 \pm 0.01 \rightarrow 1.15 \pm 0.01$	$1.68 \pm 0.01 \rightarrow 1.05 \pm 0.01$	$1.21 \pm 0.01 \rightarrow 0.95 \pm 0.01$
1321	(18.13%)	(0.89%)	(17.14%)	(18.00%)	(14.37%)	(38.46%)	(21.54%)
1322	<i>Weather</i>						
1323	$1.01 \pm 0.02 \rightarrow 0.88 \pm 0.01$	$0.83 \pm 0.02 \rightarrow 0.82 \pm 0.01$	$0.96 \pm 0.02 \rightarrow 0.86 \pm 0.01$	$0.96 \pm 0.02 \rightarrow 0.87 \pm 0.01$	$0.91 \pm 0.02 \rightarrow 0.89 \pm 0.01$	$0.93 \pm 0.02 \rightarrow 0.85 \pm 0.01$	$0.97 \pm 0.02 \rightarrow 0.87 \pm 0.01$
1324	(12.10%)	(0.04%)	(9.69%)	(9.32%)	(2.07%)	(8.54%)	(10.07%)
1325	$1.03 \pm 0.03 \rightarrow 0.90 \pm 0.02$	$0.86 \pm 0.03 \rightarrow 0.85 \pm 0.02$	$1.01 \pm 0.03 \rightarrow 0.89 \pm 0.02$	$1.01 \pm 0.03 \rightarrow 0.90 \pm 0.02$	$0.93 \pm 0.03 \rightarrow 0.90 \pm 0.02$	$0.98 \pm 0.03 \rightarrow 0.88 \pm 0.02$	$1.01 \pm 0.03 \rightarrow 0.89 \pm 0.02$
1326	(12.15%)	(0.03%)	(10.92%)	(10.80%)	(2.18%)	(9.95%)	(11.32%)
1327	$1.13 \pm 0.02 \rightarrow 0.96 \pm 0.01$	$0.87 \pm 0.02 \rightarrow 0.86 \pm 0.01$	$1.10 \pm 0.02 \rightarrow 0.95 \pm 0.01$	$1.10 \pm 0.02 \rightarrow 0.95 \pm 0.01$	$0.98 \pm 0.02 \rightarrow 0.94 \pm 0.01$	$1.06 \pm 0.02 \rightarrow 0.92 \pm 0.01$	$1.12 \pm 0.02 \rightarrow 0.96 \pm 0.01$
1328	(14.46%)	(0.002%)	(13.54%)	(13.48%)	(3.76%)	(12.43%)	(13.90%)
1329	$1.33 \pm 0.02 \rightarrow 1.08 \pm 0.01$	$0.85 \pm 0.02 \rightarrow 0.84 \pm 0.01$	$1.34 \pm 0.02 \rightarrow 1.09 \pm 0.01$	$1.34 \pm 0.02 \rightarrow 1.09 \pm 0.01$	$1.07 \pm 0.02 \rightarrow 1.00 \pm 0.01$	$1.29 \pm 0.02 \rightarrow 1.06 \pm 0.01$	$1.35 \pm 0.02 \rightarrow 1.09 \pm 0.01$
1330	(18.43%)	(0.08%)	(18.15%)	(18.24%)	(5.87%)	(17.63%)	(18.57%)
1331	$1.12 \pm 0.01 \rightarrow 0.96 \pm 0.01$	$0.85 \pm 0.01 \rightarrow 0.84 \pm 0.01$	$1.10 \pm 0.01 \rightarrow 0.95 \pm 0.01$	$1.10 \pm 0.01 \rightarrow 0.95 \pm 0.01$	$0.97 \pm 0.01 \rightarrow 0.93 \pm 0.01$	$1.06 \pm 0.01 \rightarrow 0.93 \pm 0.01$	$1.11 \pm 0.01 \rightarrow 0.95 \pm 0.01$
1332	(14.29%)	(0.03%)	(13.07%)	(12.96%)	(3.47%)	(12.13%)	(13.47%)

A.4 EXPERIMENTS ON PERFORMANCE IMPROVEMENT AS A FUNCTION OF THE NUMBER OF ACTIONS

In this section, we analyze the performance improvements achieved by post-training optimization on the *DLinear* model for the *ETTm1* dataset. Specifically, we examine how the performance varies with different prediction horizons and different numbers of actions. The results are summarized in the table below:

Table 8: Adaptive optimization improved performance.

Horizon	2 Actions	4 Actions	7 Actions
96	3.63 ± 0.54	3.74 ± 0.93	5.05 ± 0.39
192	2.10 ± 0.26	2.80 ± 0.47	3.62 ± 0.66
336	3.25 ± 0.93	3.45 ± 0.61	3.66 ± 0.71
720	2.37 ± 0.78	3.29 ± 0.47	3.97 ± 0.78

The table displays the performance improvements (in terms of error reduction) achieved through adaptive optimization at various prediction horizons (96, 192, 336, and 720) and with different numbers of actions (2, 4, and 7). The values are presented as mean \pm standard deviation, providing an indication of the variability in performance.

1350 A.5 CROSS-METRIC EVALUATION OF OPTIMIZATION STRATEGIES
1351

1352 To systematically investigate whether optimizing a single metric (e.g., Mean Squared Error, MSE)
1353 can lead to artificial or misaligned improvements in other metrics, we designed a comprehensive
1354 evaluation framework.

1355
1356 METHODOLOGY

1357 We constructed a **cross-metric evaluation matrix** with the following structure:

1359
1360 • **Rows:** Metrics used for optimization, including MSE, Mean Absolute Error (MAE), Mean
1361 Absolute Percentage Error (MAPE), and R^2 .
1362 • **Columns:** Metrics used for evaluation.

1363 For each cell, we report the **relative improvement per episode** across the training, validation, and
1364 test sets, quantifying how optimizing one metric affects the others.
1365

1366 RESULTS AND VISUALIZATION
1367

1368 Figure 12 provides a visual summary. We observe two interesting phenomena:

1369
1370 • **Consistent landscapes:** Across most optimization settings, the training, validation, and test
1371 losses share similar landscapes, indicating that overfitting is empirically mitigated. This
1372 aligns with the theoretical rationale that our small, interpretable action set limits overfitting.
1373
1374 • **Cross-metric agreement:** Improvements generalize well across metrics, confirming that
1375 our approach is not merely metric-specific gaming but delivers genuine gains across multiple
1376 evaluation criteria.
1377
1378 • **Aligned metrics:** When metrics are well-aligned, improvements generally transfer across
1379 metrics.
1380
1381 • **Incompatible metrics:** Optimization may slightly degrade performance on incompatible
1382 metrics; for example, optimizing MAPE can reduce R^2 .

1382 A.6 MORE EXPERIMENTS ON THE HUMAN FEEDBACK
1383

1384 **Detailed principle of the human in the loop framework** The system generates executable code
1385 based on user feedback using a language model (LLM). The process is as follows:

1386
1387 • **User Feedback:** The user provides a natural language description of the desired transforma-
1388 tion (e.g., scaling predictions).
1389
1390 • **Prompt Generation:** The feedback is passed through a function that creates a structured
1391 prompt for the LLM.
1392
1393 • **LLM Code Generation:** The LLM generates a Python class and function based on the
1394 feedback. The class includes a transformation function and a parameter generation function.
1395
1396 • **Optimization:** Following code generation, the system optimizes the transformation via
1397 bandit, RL or genetic algorithms to improve performance.

1398 The generated prompt is structured as follows:

```
1399 def build_feedback_prompt(feedback):  
1400     return f"""  
1401     Given the following feedback about a time series prediction model:  
1402     Feedback: "{feedback}"  
1403     Please generate a Python class called 'GenericFunction' that represents a transfor
```

1404

1405

1406

1407

1408

1409

1410

1411

1412

1413

1414

1415

1416

1417

1418

1419

1420

1421

1422

1423

1424

1425

1426

1427

1428

1429

1430

1431

1432

1433

1434

1435

1436

1437

1438

1439

1440

1441

1442

1443

1444

1445

1446

1447

1448

1449

1450

1451

1452

1453

1454

1455

1456

1457

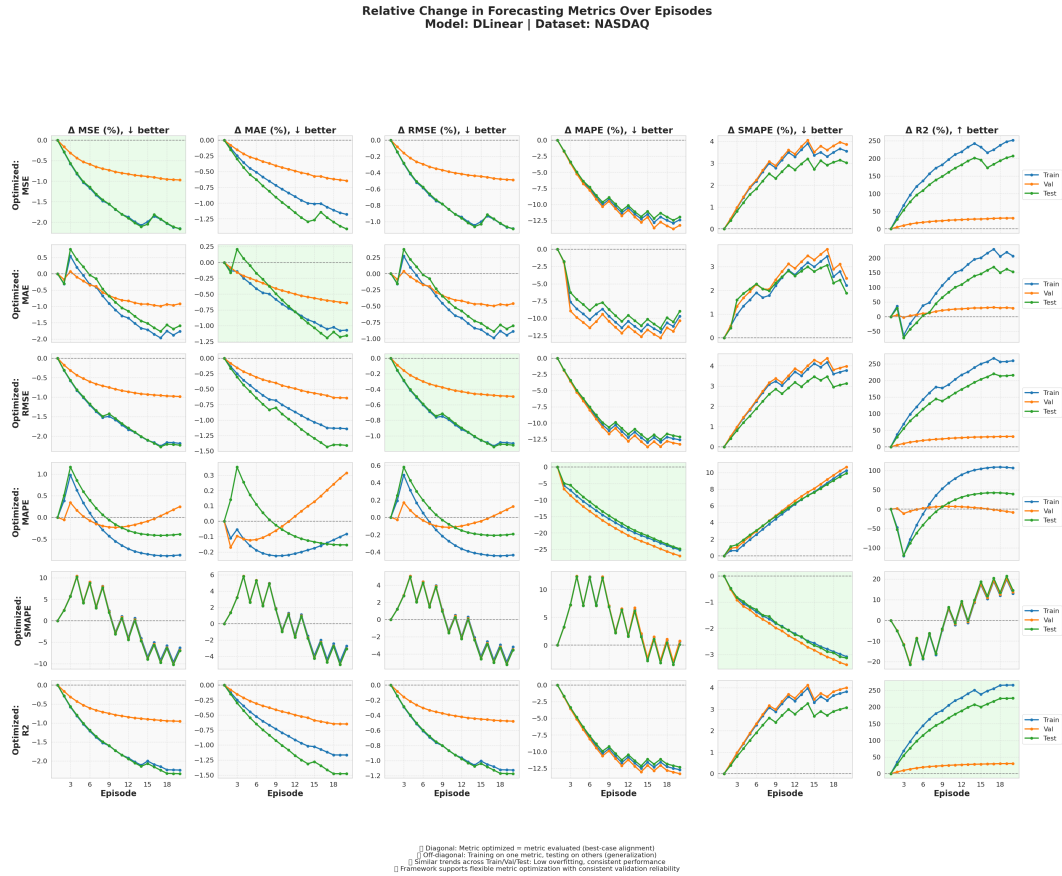


Figure 11: Cross-metric relative improvements. Rows correspond to the optimization metric, columns correspond to the evaluation metric.

1. A constructor (‘`__init__`’) that accepts:
 - ‘`function_type`’: The type of transformation.
 - ‘`params`’: A dictionary containing parameters for the transformation.

2. An ‘`apply`’ method that modifies the prediction or context vector and outputs

Additionally, generate a function ‘`generate_random_params_for_action`’ that returns

--- START OF GENERATED CODE ---

```
# Class Definition:
class GenericFunction:
<class-body>
```

```
# Function Definition:
def generate_random_params_for_action(action, batch_x):
<function-body>
```

--- END OF GENERATED CODE ---

” ” ”

The system then optimizes the generated code using the proposed optimization schemes, ensuring that the generated transformations lead to performance improvements.

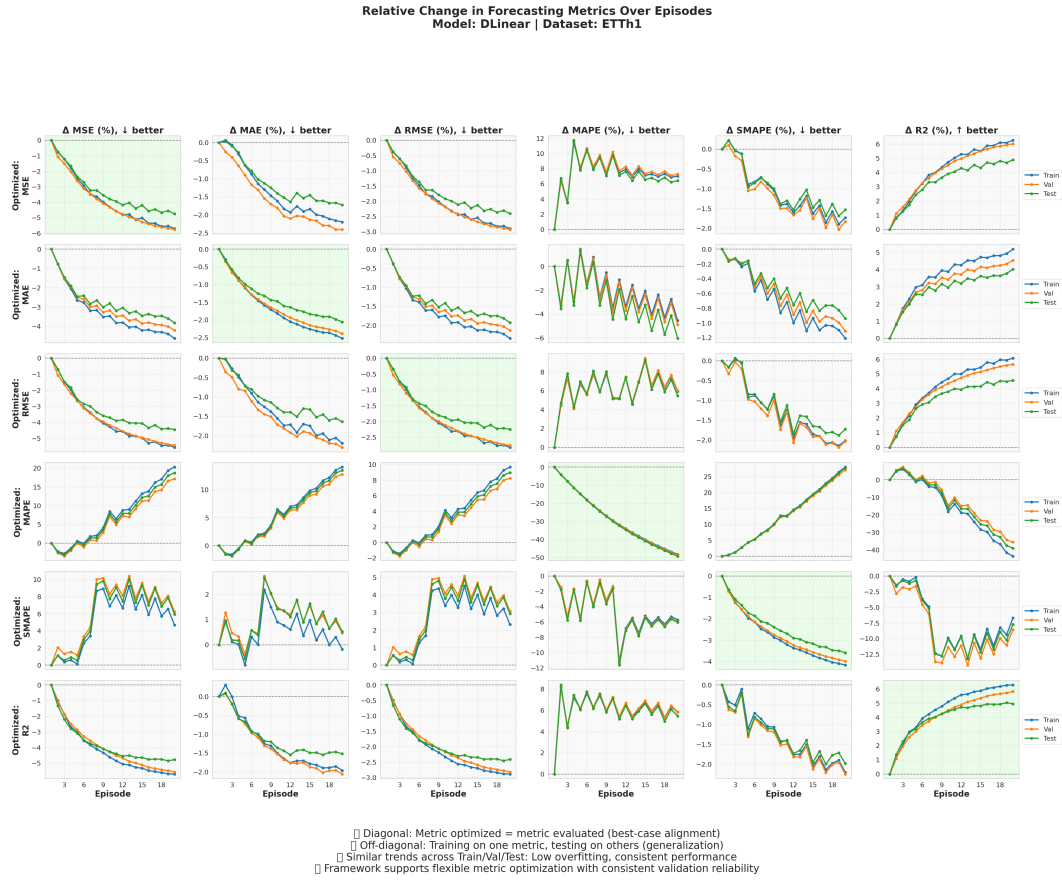


Figure 12: Cross-metric relative improvements. Rows correspond to the optimization metric, columns correspond to the evaluation metric.

A.6.1 HUMAN FEEDBACK IN ACTION

In this section, we illustrate the practical impact of human feedback through three representative examples, each consisting of a triplet of subplots. These examples demonstrate how natural language insights from a human user can be translated into targeted post-training actions, improving forecasting accuracy beyond automated optimization alone.

Each example includes the following three visualizations:

- **Forecast Comparison with Feedback Summary:** The first subplot presents the full forecasting context: the historical context vector, the model’s initial predictions, the predictions after reinforcement learning (RL)-based optimization, and the final forecast incorporating human feedback. The title of each subplot includes the specific textual instruction provided by the human. This view emphasizes how the feedback alters the forecasted trajectory.
- **Generated Code from Human Instruction:** The second subplot displays the code snippet generated by a lightweight language model (LLM) based on the human’s textual feedback. This demonstrates the interpretability and direct translatability of natural language instructions into executable post-processing transformations.
- **RMSE Improvement Visualization:** The third subplot shows the reduction in RMSE achieved by applying the human-guided correction compared to the RL-only optimization. This quantifies the value added by the human-in-the-loop mechanism.

Each of the three examples showcases a different type of human insight—such as noise reduction, trend adjustment, or outlier suppression—emphasizing both the flexibility and effectiveness of

incorporating human feedback in the post-training phase. These case studies highlight the potential of combining automated learning with domain expertise to refine time series forecasts in practice.

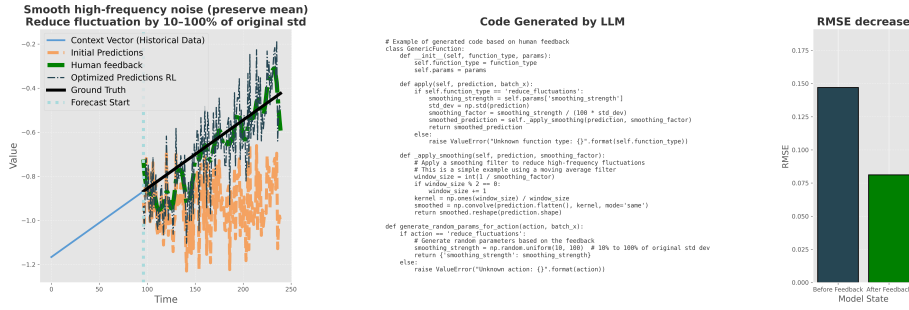


Figure 13: Human feedback integration example 1: Forecast comparison with RL and human feedback (top), code generated from human feedback (middle), and RMSE improvement (bottom).
Dataset: Dominick, **Model:** PatchTST

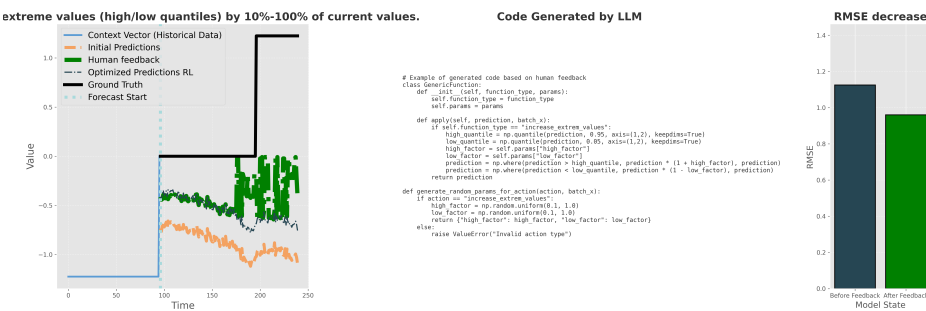


Figure 14: Human feedback integration example 2: Forecast comparison with RL and human feedback (top), code generated from human feedback (middle), and RMSE improvement (bottom).
Dataset: Nature, **Model:** DLinear

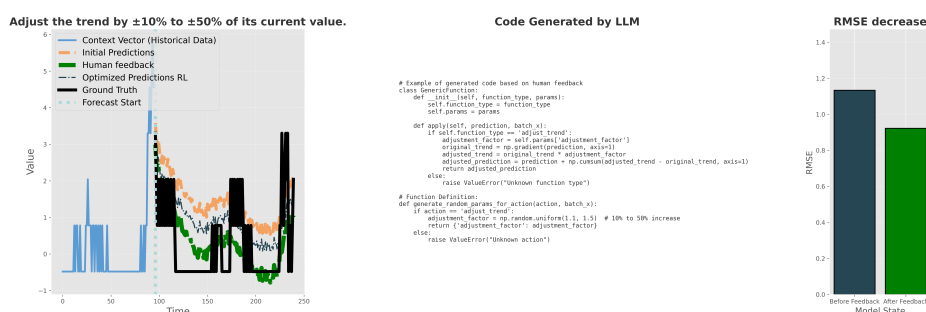


Figure 15: Human feedback integration example 3: Forecast comparison with RL and human feedback (top), code generated from human feedback (middle), and RMSE improvement (bottom).
Dataset: Tourism, **Model:** PatchTST

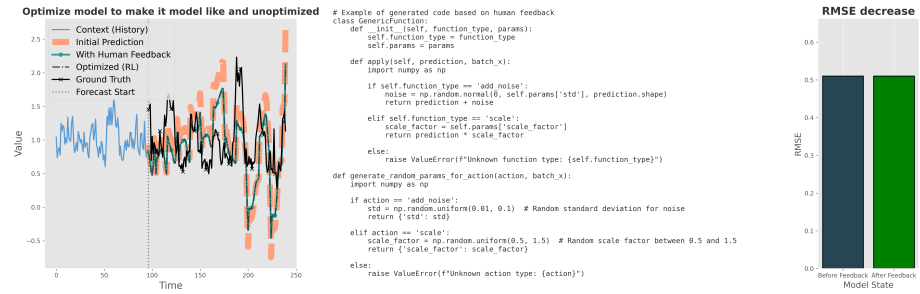
1566
1567

A.6.2 ROBUSTNESS ANALYSIS WITH RESPECT TO THE PROMPT

1568
1569
1570
1571
1572

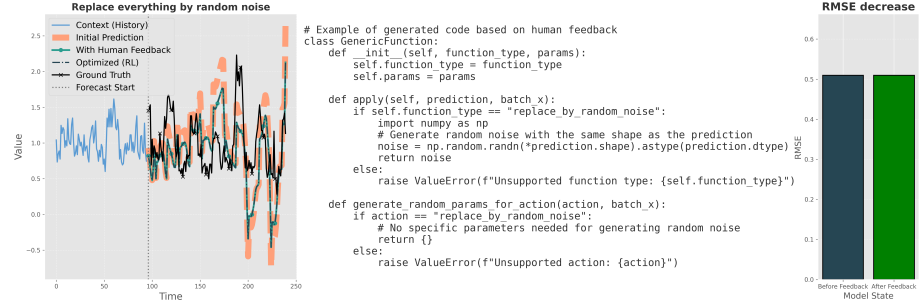
To demonstrate the robustness of the proposed framework, we analyze failure cases where the prompt is either ambiguous or nonsensical. These cases are intentionally designed to test the system's ability to handle invalid or poorly defined feedback. The framework is robust in that it identifies and discards actions that do not lead to performance improvements, ensuring that only meaningful transformations are applied.

1573
1574
1575
1576
1577
1578
1579
1580
1581
1582
1583
1584



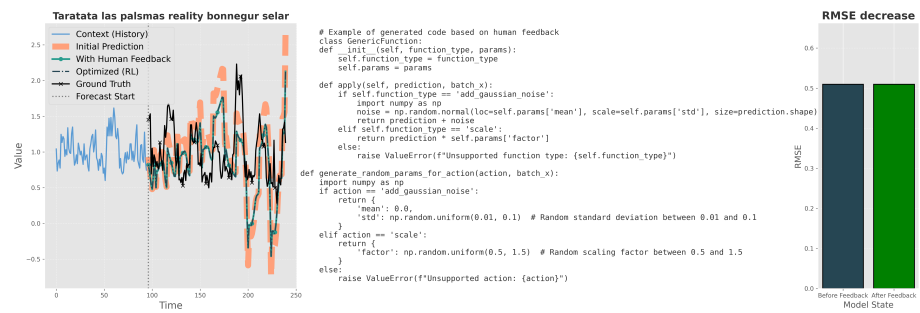
1585
1586
1587
1588
1589
1590
1591
1592
1593
1594
1595
1596
1597
1598
1599
1600

Figure 16: Human feedback integration example 4: Forecast comparison with RL and human feedback (top), code generated from human feedback (middle), and RMSE improvement (bottom).
Dataset: ETTm1, **Model:** DLinear



1601
1602
1603
1604
1605
1606
1607
1608
1609
1610
1611
1612
1613
1614
1615
1616

Figure 17: Human feedback integration example 3: Forecast comparison with RL and human feedback (top), code generated from human feedback (middle), and RMSE improvement (bottom).
Dataset: ETTm1, **Model:** DLinear



1617
1618
1619

Figure 18: Human feedback integration example 6: Forecast comparison with RL and human feedback (top), code generated from human feedback (middle), and RMSE improvement (bottom).
Dataset: ETTm1, **Model:** DLinear

1620 A.7 CODE AND REPRODUCIBILITY
1621

1622 To enable full reproducibility of our results, we provide detailed instructions for using the code
1623 associated with our framework. This section includes guidelines for setting up the environment,
1624 running the experiments, and utilizing the graphical user interface (GUI) for easy interaction with the
1625 framework. We also provide links to the repository, ensuring that interested readers can freely access
1626 and experiment with our code.

1627
1628 A.8 CODE USAGE AND API DOCUMENTATION
1629

1630 This appendix provides instructions for using the codebase and the API for time series model
1631 post-training and human feedback exploration. The framework provides a method for users to
1632 adjust model predictions using human feedback and contextual bandit algorithms, allowing the
1633 model to dynamically adapt its behavior. The code is available at https://github.com/posttraining/post_training.

1634
1635 GOAL
1636

1637 The primary goal of this project is to provide an interactive environment where users can fine-tune
1638 time series model predictions based on human feedback. The framework leverages a contextual
1639 bandit approach, allowing users to explore different actions and see their impact on the model's
1640 predictions.

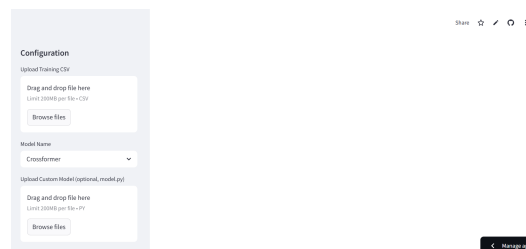
1641
1642 FEATURES
1643

- **Time Series Model Exploration:** Train and explore various time series models with different parameters and datasets.
- **Optimization Framework:** Dynamically apply actions and evaluate their effects on the model's prediction accuracy.
- **Human Feedback Integration:** Users can provide feedback on the predictions to improve the model's output over time.
- **Streamlit Interface:** An interactive frontend for exploring and providing feedback on model predictions.

1653 A.8.1 EXAMPLES TO USE THE STREAMLIT APPLICATION
1654

1655 To experiment with the Streamlit application, follow these steps:

1656
1657 1. **Click on the following (link):** Go to the webpage. You should see the configuration page as
1658 in Figure 19.



1659
1660 Figure 19: Configuration page
1661
1662
1663
1664
1665
1666
1667
1668
1669
1670

1671 2. **Upload CSV File:** Upload a CSV file containing the time series data. The file should
1672 be in CSV format, with rows representing different time steps and columns representing
1673 different features for multivariate datasets. A sample file, `train.csv`, is provided in the
supplementary materials. You can see an example in Figure 20

```
1674  
1675  
1676  
1677  
1678  
1679  
1680  
1681  
1682  
1683
```

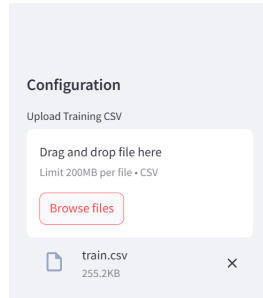


Figure 20: Example of upload file

```
1684  
1685  
1686  
1687 3. Select Model and Options: Choose the model and other options. For the model, use  
1688 DLinear, as other models require a GPU to run or will take longer. The server currently  
1689 supports CPU only as in Figure 21  
1690
```

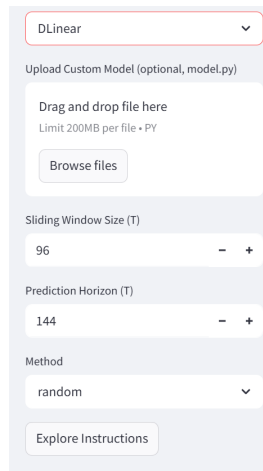


Figure 21: Configuration Options

```
1706  
1707  
1708  
1709 4. Explore Instructions: Click on the "Explore Instructions" button. After some time, you  
1710 will see the optimization process (with the successful actions over the episodes) as in Figure  
1711 22 and the reduced MSE after each episode on the validation set as in Figure 23  
1712
```

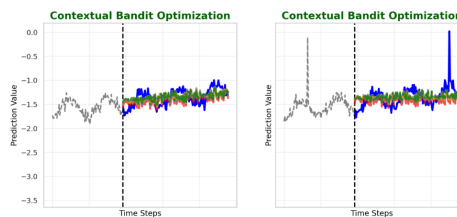


Figure 22: Successfull and failed actions during optimization

```
1713  
1714  
1715  
1716  
1717  
1718  
1719  
1720  
1721  
1722  
1723 5. Provide Feedback: Enter your feedback in text, in any language. Be as descriptive as  
1724 possible to guide the model. For example, you could say, "The amplitude of the predictions  
1725 should be increased between 5% and 10% of the actual values." as in Figure 24  
1726  
1727 6. Submit Feedback: Click on "Submit Feedback" and then "Finalize Feedback." You will  
see the percentage improvement and details per channel as in Figure 25
```

1728
1729
1730
1731
1732
1733
1734
1735
1736
1737
1738
1739
1740

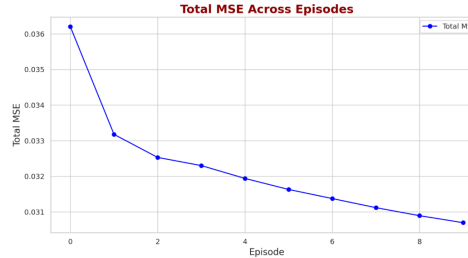


Figure 23: MSE as function of the number of episodes

1741
1742
1743
1744
1745
1746
1747
1748
1749
1750

Provide Feedback

Enter your feedback

The amplitude of the predictions should be increased between 5% and 10% of the actual values

Press Ctrl+Enter to apply

1751
1752
1753
1754
1755
1756
1757

Figure 24: Example of user prompt

1758
1759
1760
1761
1762
1763
1764
1765
1766

```
### MSE Improvement Summary
- **Total Initial MSE**: 0.0502
- **Total Final MSE**: 0.0308
- **Total Improvement**: 0.0194
- **Overall MSE Improvement**: 38.70%

**Channel-wise MSE Improvements**:
• Channel 1: 0.0188 MSE
• Channel 2: 0.0166 MSE
• Channel 3: 0.0193 MSE
• Channel 4: 0.0225 MSE
• Channel 5: 0.0196 MSE
• Channel 6: 0.0214 MSE
• Channel 7: 0.0180 MSE
```

Figure 25: Improvement Details

1767
1768
1769
1770
1771
1772
1773
1774
1775
1776
1777
1778
1779
1780
1781

1782 A.9 INSTALLATION AND USAGE FOR DEVELOPMENT
1783

1784 INSTALLATION INSTRUCTIONS

1785 **Set Up the Environment** To install the required dependencies, create and activate the conda
1786 environment:

1788 conda env create -f environment.yml
1789

1790 USAGE
1791

1792 **Running the Code with Command-Line Arguments** To run the post-training process and adjust
1793 the model, execute the following command:

1794
1795 python main.py --train_path <path_to_train_data
1796 --model <model_name> --window_size <window_size> --prediction_horizon <prediction_ho
1797 --batch_size <batch_size> --n_samples <n_samples>

1798 The available command-line arguments are as follows:
1799

Argument	Description	Example
-train_path	Path to the training data CSV file	data/train.csv
-model	Name of the model to use	DLinear, PatchTST, etc.
-model_path	(Optional) Path to a custom pre-trained model	models/custom_model.py
-window_size	Sliding window size for time series	96
-prediction_horizon	Prediction horizon in terms of time steps	144
-batch_size	Batch size for training	32
-n-jobs	Number of CPU for parallel computing	1
-episodes	Number of episodes for RL training	5

1800
1801 **Running the Streamlit App** To interact with the framework using the Streamlit interface, launch
1802 the app as follows:
1803

1804 streamlit run app_test.py
1805

1806 This will start a local server, and you can access the interface by navigating to the URL provided in
1807 the terminal.
1808

1809 **Workflow Overview** The following steps outline the workflow of the post-training process:
1810

1. **Train the Model:** Train the model using the provided training data and validate it using the
1821 validation dataset. Optionally, load a custom pre-trained model if specified.
2. **Exploration Phase:** After training, explore various actions on top of the model's predictions.
1823 These actions include adjusting amplitudes, trends, or shifting values.
3. **Human Feedback:** Provide feedback on the predictions to guide the model towards im-
1825 provements. Precise feedback, such as "increase the amplitude by 5-10%", allows the model
1826 to understand the desired adjustments.
4. **Model Adaptation:** Based on the feedback, the model adapts its behavior and re-tests the
1829 adjusted predictions.
5. **Plotting Results:** The results of the model's predictions are visualized through plots, which
1831 are saved for further analysis.

1832 **API Documentation** The API for the framework is structured as follows:
1833

1. app_test.py: Main script to run the Streamlit interface. Provides functionalities to
1835 explore and give feedback on model predictions.

1836 2. `contextual_bandit.py`: Implements the contextual bandit logic for dynamically
 1837 adjusting predictions based on feedback.
 1838 3. `data_extraction.py`: Contains functions for loading and preprocessing time series
 1839 data.
 1840 4. `llm_interaction.py`: Functions for interacting with language models to interpret and
 1841 apply human feedback.
 1842 5. `model_extraction.py`: Extracts and loads pre-trained models.
 1843 6. `plot_script.py`: Provides plotting utilities for visualizing predictions and feedback
 1844 results.
 1845

1846

1847 A.10 THEORETICAL MOTIVATION FOR POST TRAINING IN TIME SERIES FORECASTING

1848

1849 A.10.1 PROBLEM SETUP

1850

1851 Consider a supervised learning problem where we want to estimate a target variable Y_{true} using a
 1852 linear model. We assume that a ridge regression predictor Y_{pred} has already been obtained, and we
 1853 aim to improve its accuracy through an optimal affine correction of the form:

1854

$$Y_{\text{corrected}} = aY_{\text{pred}} + b. \quad (3)$$

1855

1856 The goal is to determine the optimal values of a and b that minimize the expected mean squared error
 1857 (MSE):

1858

$$\mathcal{L}(a, b) = \mathbb{E} [\|Y_{\text{true}} - (aY_{\text{pred}} + b)\|^2]. \quad (4)$$

1859

1860 A.10.2 DERIVATION OF OPTIMAL CORRECTION PARAMETERS

1861

1862 Expanding the loss function:

1863

$$\mathcal{L}(a, b) = \mathbb{E} [Y_{\text{true}}^2 - 2aY_{\text{true}}Y_{\text{pred}} - 2bY_{\text{true}} + a^2Y_{\text{pred}}^2 + 2abY_{\text{pred}} + b^2]. \quad (5)$$

1864

1865 **Step 1: Compute b^* by setting $\frac{\partial \mathcal{L}}{\partial b} = 0$.**

1866

$$\frac{\partial \mathcal{L}}{\partial b} = -2\mathbb{E}[Y_{\text{true}}] + 2a\mathbb{E}[Y_{\text{pred}}] + 2b. \quad (6)$$

1867

1868 Setting this derivative to zero and solving for b^* gives:

1869

$$b^* = \mathbb{E}[Y_{\text{true}}] - a^*\mathbb{E}[Y_{\text{pred}}]. \quad (7)$$

1870

1871 **Step 2: Compute a^* by setting $\frac{\partial \mathcal{L}}{\partial a} = 0$.**

1872

$$\frac{\partial \mathcal{L}}{\partial a} = -2\mathbb{E}[Y_{\text{true}}Y_{\text{pred}}] + 2a\mathbb{E}[Y_{\text{pred}}^2] + 2b\mathbb{E}[Y_{\text{pred}}]. \quad (8)$$

1873

1874 Substituting b^* and solving for a^* gives:

1875

$$a^* = \frac{\text{Cov}(Y_{\text{true}}, Y_{\text{pred}})}{\text{Var}(Y_{\text{pred}})}. \quad (9)$$

1876

1877 Thus, the optimal correction parameters are:

1878

$$a^* = \frac{\mathbb{E}[(Y_{\text{true}} - \mathbb{E}[Y_{\text{true}}])(Y_{\text{pred}} - \mathbb{E}[Y_{\text{pred}}])]}{\mathbb{E}[(Y_{\text{pred}} - \mathbb{E}[Y_{\text{pred}}])^2]}, \quad (10)$$

1879

$$b^* = \mathbb{E}[Y_{\text{true}}] - a^*\mathbb{E}[Y_{\text{pred}}]. \quad (11)$$

1880

1881 A.10.3 THEORETICAL RISK BEFORE AND AFTER CORRECTION

1882

1883 **Risk Before Correction:** The mean squared error (MSE) of the original predictor is given by:

1884

$$R_{\text{before}} = \mathbb{E}[(Y_{\text{true}} - Y_{\text{pred}})^2]. \quad (12)$$

1885

1886 Expanding:

1887

$$R_{\text{before}} = \text{Var}(Y_{\text{true}}) + \text{Var}(Y_{\text{pred}}) - 2\text{Cov}(Y_{\text{true}}, Y_{\text{pred}}). \quad (13)$$

1888

1890 **Risk After Correction:** The mean squared error of the optimally corrected predictor is:

$$1891 \quad 1892 \quad R_{\text{after}} = \mathbb{E}[(Y_{\text{true}} - Y_{\text{corrected}})^2]. \quad (14)$$

1893 Substituting $Y_{\text{corrected}} = a^* Y_{\text{pred}} + b^*$:

$$1894 \quad 1895 \quad R_{\text{after}} = \text{Var}(Y_{\text{true}}) - \frac{\text{Cov}(Y_{\text{true}}, Y_{\text{pred}})^2}{\text{Var}(Y_{\text{pred}})}. \quad (15)$$

1897 A.10.4 COMPARISON OF RISKS

1899 To understand the effect of the correction, we compute the difference:

$$1900 \quad 1901 \quad R_{\text{before}} - R_{\text{after}}. \quad (16)$$

1902 Substituting the expressions:

$$1904 \quad R_{\text{before}} - R_{\text{after}} = [\text{Var}(Y_{\text{true}}) + \text{Var}(Y_{\text{pred}}) - 2\text{Cov}(Y_{\text{true}}, Y_{\text{pred}})] \\ 1905 \quad - \left[\text{Var}(Y_{\text{true}}) - \frac{\text{Cov}(Y_{\text{true}}, Y_{\text{pred}})^2}{\text{Var}(Y_{\text{pred}})} \right]. \quad (17)$$

1907 Simplifying:

$$1909 \quad 1910 \quad R_{\text{before}} - R_{\text{after}} = \text{Var}(Y_{\text{pred}}) - 2\text{Cov}(Y_{\text{true}}, Y_{\text{pred}}) + \frac{\text{Cov}(Y_{\text{true}}, Y_{\text{pred}})^2}{\text{Var}(Y_{\text{pred}})}. \quad (18)$$

1912 Rewriting using the identity:

$$1914 \quad \left(x - \frac{a}{x} \right)^2 \geq 0 \quad \text{for all } x > 0, \quad (19)$$

1915 by setting $x = \text{Var}(Y_{\text{pred}})$ and $a = \text{Cov}(Y_{\text{true}}, Y_{\text{pred}})^2$, we obtain:

$$1917 \quad 1918 \quad R_{\text{before}} - R_{\text{after}} = \left(\sqrt{\text{Var}(Y_{\text{pred}})} - \frac{\text{Cov}(Y_{\text{true}}, Y_{\text{pred}})}{\sqrt{\text{Var}(Y_{\text{pred}})}} \right)^2. \quad (20)$$

1920 Since the square of any real number is always non-negative:

$$1922 \quad R_{\text{before}} - R_{\text{after}} \geq 0. \quad (21)$$

1924 A.10.5 CONCLUSION

1925 This derivation shows that the correction always reduces the risk (or at worst, leaves it unchanged).
1926 The correction is most effective when Y_{pred} is correlated with Y_{true} , and it does not increase the error
1927 in any case. This result shows that the correction always reduces the mean squared error.

1929 A.11 PROOF OF THE *Upper Bound on the Risk of the Corrected Prediction THEOREM*

1931 For completeness we give here the general theorem (for $K > 2$) and its assumptions.

1933 **Assumption 1 (Gaussian Squared-Error Model)** For all indices k , hyperparameters β , and the
1934 base model f_θ , we assume that for $(X, Y) \sim \mathcal{D}$,

1935 $((g_{k,\beta} \circ f_\theta)(X) - Y)^2$ follows a Gaussian distribution with mean $R(g_{k,\beta} \circ f_\theta)$ and variance $\sigma^2 > 0$.

1937 This provides a convenient concentration model for the empirical risk estimates used by the algorithm.

1939 **Theorem 2 (Upper Bound on the Risk of the Corrected Prediction)** Let f_θ be a base predictor,
1940 $(g_{k,\beta^*})_{k=1}^K$ a set of corrective actions, and assume a total evaluation budget T under $M = 1$.
1941 Under [Assumption 1](#), applying Successive Halving to select a correction yields:

$$1942 \quad 1943 \quad \mathbb{E}[R(g_{k_T, \beta^*} \circ f_\theta)] \leq \frac{1}{\nu} \sum_{k=1}^K \bar{R}(k) \prod_{r=0}^{\log_2 K-1} \left[(k-1) \Phi(-\Delta_{\min, k}^+ \tau_{\text{dec}}(r)) + (K-k) \Phi(-\Delta_{\min, k}^- \tau_{\text{inc}}(r)) \right],$$

1944 where

$$\begin{aligned}
 1945 \quad \bar{R}(k) &:= \min\{R(f_\theta), R(g_{k,\beta^*} \circ f_\theta)\}, \quad \nu := \frac{K^{\log_2 K}}{2\sqrt{2^{\log_2 K(\log_2 K+1)}}}, \\
 1946 \quad \tau_{\text{dec}}(r) &:= \sqrt{\frac{T2^r}{2\sigma^2 K \log_2 K} - \frac{1}{2\sigma^2}}, \quad \tau_{\text{inc}}(r) := \sqrt{\frac{T2^r}{2\sigma^2(K \log_2 K - 2^r \log_2 K)}}, \\
 1947 \quad \Delta_{\min,k}^+ &:= \min_{\substack{j \neq k \\ R(k) > R(j)}} (R(k) - R(j)), \quad \Delta_{\min,k}^- := \min_{\substack{j \neq k \\ R(k) < R(j)}} (R(k) - R(j)).
 \end{aligned}$$

1953 **Proof 1 (Sketch of the proof)** We provide here a self-contained outline; the full derivation follows
 1954 the style of [Karnin et al. \(2013\)](#) for Successive Halving.

1956 **Step 1: Decomposition.** Each corrective action g_{k,β^*} has a fixed true risk $R(g_{k,\beta^*} \circ f_\theta)$. Only the
 1957 index k_T selected by the algorithm is random because it depends on noisy empirical risk estimates.
 1958 Hence,

$$\begin{aligned}
 1959 \quad \mathbb{E}[R(g_{k_T,\beta^*} \circ f_\theta)] &= \sum_{k=1}^K \min(R(f_\theta), R(g_{k,\beta^*} \circ f_\theta)) \mathbb{P}[k_T = k]. \\
 1960 \\
 1961
 \end{aligned}$$

1962 **Step 2: Bounding the selection probability.** Successive Halving proceeds over $n_r = \log_2 K$ rounds.
 1963 At round r , each remaining action in the set S_r is evaluated t_r times and half of them are discarded.
 1964 For a fixed k , the number of competing actions with lower empirical risk than k can be expressed as
 1965 a sum of Bernoulli variables whose expectations are Gaussian tail probabilities:

$$\mathbb{E}[N_{r,k}] = \sum_{j \neq k} \Phi\left(-\frac{\Delta_{k,j} \sqrt{t_r}}{\sqrt{2}\sigma}\right).$$

1966 Using Markov's inequality and introducing the smallest positive and negative risk gaps $\Delta_{\min,k}^+$ and
 1967 $\Delta_{\min,k}^-$, we obtain a product-form upper bound on $\mathbb{P}[k_T = k]$ across all rounds.

1972 **Step 3: Plug into the risk expression.** Substituting this bound on $\mathbb{P}[k_T = k]$ into the decomposition
 1973 above yields the stated inequality.

1975 **Discussion.** This theorem formalizes how Successive Halving selects the best correction under
 1976 limited evaluation budget. The bound shows that the expected risk converges to the risk of the optimal
 1977 correction at an exponentially fast rate, with the convergence speed determined by the risk gaps
 1978 $\Delta_{\min,k}^\pm$ and the budget T . In particular, larger gaps between actions accelerate the identification of
 1979 the optimal correction—exactly mirroring the empirical behavior observed in our experiments.

1980
 1981
 1982
 1983
 1984
 1985
 1986
 1987
 1988
 1989
 1990
 1991
 1992
 1993
 1994
 1995
 1996
 1997